AD NUMBER

AD853537

LIMITATION CHANGES

TO:

Approved for public release; distribution is unlimited.

FROM:

Distribution authorized to U.S. Gov't. agencies and their contractors; Critical Technology; APR 1969. Other requests shall be referred to U.S. Army Missile Command, Redstone Arsenal, AL 35809. This document contains export-controlled technical data.

AUTHORITY

USAMC ltr, 29 Nov 1972

AD

REPORT NO. RE-TR-69-9

A MODEL FOR THE SPECTRAL EMISSIVITY OF CARBON DIOXIDE IN THE 4.3-MICRON BAND

by

H. Tracy Jackson, Jr.

April 1969

U.S. ARMY MISSILE COMMAND
Redstone Arsenal, Alabama

DISPOSITION INSTRUCTIONS

Destroy this report when it is no longer needed. Do not return it to the originator.

DISCLAIMER

The findings in this report are not to be construed as an official Department of the Army position unless so designated by other authorized documents.

TRADE NAMES

Use of trade names or manufacturers in this report does not constitute an official indorsement or approval of the use of such commercial hardware or software.

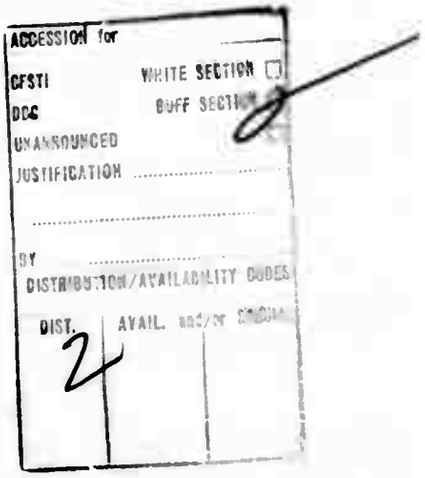

7 April 1969

Report No. RE-TR-69-9

A MODEL FOR THE SPECTRAL EMISSIVITY OF CARBON DIOXIDE IN THE 4.3-MICRON BAND

by

H. Tracy Jackson, Jr.

DA Project No. 1522901A204
AMC Management Structure Code No. 5221.11.146

Electro-Optical Branch
Advanced Sensors Laboratory
Research and Engineering Directorate (Provisional)
U. S. Army Missile Command
Redstone Arsenal, Alabama 35809

ABSTRACT

This report describes in somewhat tutorial detail a method for computing the spectral emissivity of hot carbon dioxide in the 4.3-micron band. This band is taken to cover the spectral region 2050 to 2400 cm^{-1} (4.17 to 4.88 microns). Data are presented for the temperature range 300° to 2100°K. Spectroscopic band parameters have largely been taken from available literature data. The average values for the integrated intensity of a rotational line (S) and the distance between the spectral lines (d) are tabulated in the standard form S/d and $S^{1/2}/d$. Values are listed every 5 cm^{-1} in increments of 300°K.

Emissivities are calculated by the statistical model. A curve of growth function suggested by Malkmus and adopted by Ben-Aryeh is used for the relationship between absorption and reduced path lengths. The results of this model agree most favorably with reliable experimental measurements.

The discussion includes homogeneous as well as inhomogeneous gases. The homogeneous case is presented in its entirety in that the emissivity model, the molecular band parameters, and the digital computer program are presented. Illustrative examples are given for both the homogeneous and inhomogeneous formulations.

CONTENTS

ILLUSTRATIONS

Table

Figure

Section I. INTRODUCTION

This report presents the results of the first phase of a program which was undertaken to analytically predict the spectral and spatial distribution of radiation emitted from an inhomogeneous, noniso-thermal system of hot gases. The program was initiated because of current interest in being able to predict the radiant power emitted by a particular system of hot gases in narrow bands of the infrared spectrum. Consequently, a study was undertaken to compile available data on the infrared spectra of certain polyatomic molecules. This report discusses the radiation from heated carbon dioxide in the vicinity of the 4.3-micron region.

In particular, this report presents the results of the initial phase of the study which was undertaken to calculate the spectral emissivity of gaseous CO_2. Results are reported for the infrared 4.3-micron band which is assumed to cover the spectral region 2050 to 2400 cm^{-1} (4.17 to 4.88 microns).* The temperature range considered was 300° to 2100°K. No extensive effort has been made to present any original results in this report, but rather a compilation of existing data was unified to construct a single spectral emission model. However, since a single model was desired to represent the emissivity over a considerable range of varying conditions, molecular band parameters had to be derived for the lower temperature range.

The primary purpose of this work was to develop a method for predicting the radiant intensity emitted from a system of hot gases where CO_2 is the dominant radiating species of the 4.3-micron spectral region. In addition, a salient feature of the program was to develop a computerized computational scheme which could be readily integrated into a flow-field calculation. Such a program would then provide both the spectral and spatial intensity distribution of the emitted radiation.

It is well established that both experimental and theoretical studies of gaseous radiation are of practical interest and importance in many problems. The radiation from hot gases generally has a spectral distribution which is quite different from the continuous blackbody Planckian spectrum. In order to calculate the radiant flux emitted from a hot gas in a particular region of the spectrum, it is necessary to integrate the spectral emittance over the desired wavelength region.

*This spectral region also covers the weak 4.8-micron (2075 cm^{-1}) band. It is important only for high values of CO_2 concentration.

The calculation of the spectral emittance involves a detailed knowledge of the emissivity of the gas. The spectral emissivity, in turn, is a very strong function of the gas temperature (assumed to be in thermal equilibrium), pressure, composition, and concentration* of the component species as well as the spectral region of interest. Obviously, the complexity of the calculation is further enhanced by the presence of varying thermal and concentration properties within the gaseous system.

In addition, it is also recognized that purely theoretical calculations (even for constant-property systems) which attempt to describe the spectral emission from a molecular band are difficult to formulate because the necessary molecular parameters are not completely known. These molecular parameters must serve as inputs to highly idealized models which, in order to be computationally tractable, are frequently not completely capable of describing a complex spectrum. Nonetheless, a large number of molecular species has received a great deal of attention during the past several years,† and various models do exist for correlating theoretical predictions with experimental measurements. A number of these band models will be discussed in Section II.

---

*In this report, the general practice of expressing concentration in terms of partial pressure will be adherred to rather than in terms of radiating particle density.

†For an early exposition of the methods which may be used to study the infrared spectral of polyatomic molecules, refer to D. M. Dennison's rather lengthy article, "The Infrared Spectra of Polyatomic Molecules," Rev. Mod. Phys. 3, 280 (1931). He does not discuss electronic states, but considers the vibrational, rotational, and symmetrical properties in a logical order. For a more modern discussion which requires no prior knowledge of quantum mechanics, see the very readable text by G. M. Barrow, Introduction to Molecular Spectroscopy, McGraw-Hill Book Co., Inc., New York, San Francisco, Toronto, and London (1962). For the serious spectroscopist, there are the two familiar texts by (1) S. S. Penner, Quantitative Molecular Spectroscopy and Gas Emissivities, Addison-Wesley Publishing Co., Inc., Reading, Massachusetts (1959), whose notation is at times atrocious and frequently varies between chapters; and (2) G. Herzberg, Spectra of Diatomic Molecules, D. Van Nostrand Co, Inc., Princeton, New Jersey; New York; Toronto; and London (1950). This is applicable since the 2350 cm^{-1} triatomic CO_2 band is parallel, resulting in the vibrational-rotational selection rules being the same as the diatomic molecules.

Carbon dioxide is a linear, symmetrical, triatomic molecule. The radiation emitted by this molecule is due to transitions from excited vibrational-rotational states to states of lower energy. Being triatomic, the CO_2 molecule has three fundamental modes of vibration. It possesses two extremely strong bands (Ref. 1) at 667 and 2349 cm^{-1}. One strong band at 1340 cm^{-1} has been found in the Raman spectrum (Ref. 1).

A linear molecule like CO_2 has two kinds of vibrational-rotational bands. When the vibration of the oscillating dipole moment is parallel to the molecular axis, certain selection rules for the various transitions arise, and the particular band is called a parallel band. However, if the vibration is such that the oscillating dipole moment is perpendicular to the molecular axis, different selection rules arise, and the rotational-vibrational band is called a perpendicular band.

The band at 2349 cm^{-1} for the CO_2 molecule is a parallel band; i. e., the oscillating dipole moment connected with the vibration is parallel to the molecular axis. This results in the vibrational-rotational selection rules being the same as the simplier diatomic molecules; namely,* $\Delta\nu = \pm 1$, $\Delta J = \pm 1$. Thus, the band will have P and R branches ($\Delta J = -1$, $\Delta J = +1$, respectively), but no Q branch ($\Delta J = 0$) or else a very weak Q branch. However, from a practical viewpoint, there is one important difference between the CO_2 molecule and the simpler diatomic molecules. The number of transitions which must be considered increases approximately as T^4 (temperature) for CO_2 as opposed to approximately T for diatomic molecules. In a recent calculation (Ref. 2), for example, some 500 transitions had to be considered in order to determine the band parameters for CO_2 in the vicinity of 2000°K.

*A quantum-mechanical description for the allowable rotational energies of a rigid rotator is $E_J = (h^2/8\pi^2 I)J(J+1)$, where I is the moment of inertia and $J = 0, 1, 2\ldots$. The allowable vibrational energies for a harmonic oscillator are $E_\nu = (\nu + \frac{1}{2})h\omega$, where ω is the frequency with which the system would vibrate if it behaved classically; $\nu = 0, 1, 2, \ldots$; and h is Planck's constant.

Section II. EMISSION MODEL

A number of studies has been undertaken in an attempt to formulate a mathematical model which describes the physical laws governing the emission of radiation from hot gases (Refs. 2 and 3).* These mathematical models are developed by assuming particular spectral distribution functions for the line intensities, line spacings, and line widths. The various models which exist for the calculation of spectral emissivities, therefore, made use of three spectroscopic band parameters generally denoted S, d, and α. S is the average integrated intensity of a rotational line, d is the average distance between spectral lines, and α is the line half-width (one-half the line width measured at one-half the maximum intensity point).

The number of spectral lines contributing to a given band increases with temperature because of thermal excitation. Since this results in a large number of transitions, it becomes impractical to consider each individual transition and the corresponding set of band parameters. For this reason, an average spectral interval can be chosen; and the individual parameters over this interval may then be reduced to a single set of average parameters. This, then, is the interpretation to be placed on the above-mentioned band parameters–namely, S, d, and α.

Since an increase in temperature increases the probability of population for the higher energy levels, then the above parameters have a significant temperature dependence. Various other conditions also influence the emission characteristics of the gas. These parameters are the pressure of the absorbing gas P, the equivalent pressure (Ref. 4)† of the gaseous mixture P_e, the optical path or thickness L, and the equivalent optical path which, for a homogeneous gas, is $L_e = PL/P_e$. The equivalent optical path–sometimes referred to as

---

*An excellent theoretical study of the various band models has been carried out by Plass in Ref. 2 (for a parallel discussion, also see his discussion in Chapter 6 of Ref. 3). Plass discusses thoroughly the regions of validity for the various approximations and compares predictions made by the different models.

†The relationship between the equivalent pressure, the total pressure, and the partial pressure of CO_2 in binary N_2 has been discussed by Burch et. al. in Ref. 4. It was shown that $P_e = P_T + 0.3\, P_{CO_2}$. Thus, for small concentrations of CO_2, the total and equivalent pressure can be assumed equal. This assumption will be made throughout this report.

the reduced optical path, optical depth, or reduced path thickness—is then defined as $L_e = P_{CO_2} L / P_T$, where P_{CO_2} is the partial pressure of CO_2 contained within a gaseous mixture whose total pressure is P_T.

No attempt is made to discuss the methods used for calculating the parameters S and d. Details can be found in Refs. 5, 6, 7, and 8. These two band model parameters are presented in this report as the ratios S/d and $S^{\frac{1}{2}}/d$. An average line half-width of 0.075 cm^{-1} at unit pressure was used at 300°K and taken to be proportional to $T^{-\frac{1}{2}}$.

Obviously, the main problem confronting this phase of the analytical study was the careful selection of both band parameters and an emission model that would realistically predict spectral emissivities over a relatively wide range of varying conditions. Since most band models are valid only for a limited range of temperature, composition, pressure, and optical path, then a model was desired which could be forced to agree with spectroscopic measurements over all ranges of interest. The study of gases in emission or absorption is generally carried out under carefully controlled conditions, whereby the temperature, pressures, concentrations, etc., are well defined. Thus, for a given band model which is assumed to represent the emissivity, the model can, within mathematical constraints, be forced to agree with measured data by carefully redefining the band parameters. Obviously, the band parameters can lose any physical significance attached to their original meaning when they undergo such a redefinition. However, this is of no consequence in a model study such as this where the ultimate criterion for the model is agreement with reliable experimental data. Still the analytical or modeling procedure must solve the theoretical problem of expressing spectral emissivities in terms of the band parameters and gas properties. Again, for fixed physically meaningful band parameters, the theorist is hard pressed to construct a single tractable analytical band model capable of describing a complex spectrum over a wide range of conditions. It has been pointed out, for example, that a given experimentally observed value of absorptance (or transmittance) may be represented by an infinite number of combinations of the band parameters. This study, therefore, proceeded with the philosophy that physically meaningful band parameters were not a constraint to be placed upon the final solution, but rather a tractable model capable of describing observed spectra.

Plass (Ref. 2) has given a detailed description of existing band model theories. The models most widely used for predicting band absorption are: 1) Elsasser model, 2) quasirandom model, 3) random Elsasser model, and 4) statistical or Mayer-Goody model.

The Elsasser model is constructed by simply allowing a given spectral line to periodically repeat itself over an interval $\Delta\nu$. Thus, the lines are evenly spaced, and each has the same intensity. It is, of course, not physically realistic to represent certain radiating systems by this type of model when the system contains many unequally spaced lines of varying intensities. The random Elsasser is simply a random superposition of two or more different Elsasser bands. The statistical model assumes that both the position and intensity of the individual lines are distributed at random and that there is no correlation between line position and intensity. The quasirandom model is the most sophisticated of these models and probably the most accurate. This model has the feature of representing the absorption by lines which are not arranged in a regular or a random manner. It can, therefore, represent an ordering of the lines that is neither as regular as the Elsasser model nor as random as the statistical model. Data from this model (Ref. 7) (quasirandom) were used to derive the band model parameters for the CO_2 at the low temperatures. These parameters were then used in the statistical model for predicting CO_2 emissivities.

Section III. MODEL DEVELOPMENT

We now consider the absorption of radiation over a wavenumber interval, $\Delta\nu$. The decrease of the spectral intensity $dI(X, \nu)$ lost by a single line in traversing a differential thickness dX of a gas is proportional to dX, the incident intensity $I(X, \nu)$ and the concentration $C(X)$ of the absorbing species. This is denoted by the usual equation

$$dI(X, \nu) \propto - I(X, \nu)C(X)dX, \tag{1}$$

where the negative sign indicates a decrease in intensity for increasing X. The proportionality constant $K(X, \nu)$ which makes the above expression an equality is called the absorption coefficient. Integration over a finite thickness L gives the transmission τ,

$$\frac{I(L, \nu)}{I(0, \nu)} = \tau(L, \nu) = \exp - \left[\int_0^L K(X, \nu)C(X)dX\right]. \tag{2}$$

Over the finite wavenumber interval $\Delta\nu$, the average transmission is given by

$$\langle\tau(L, \nu)\rangle = \frac{1}{\Delta\nu} \int_{\Delta\nu}\left\{\exp - \left[\int_0^L K(X, \nu)C(X)dX\right]\right\}d\nu. \tag{3}$$

Assuming $K(X, \nu) = K(\nu)$ and denoting the integral in the argument of the exponential by u, then this may be written

$$\langle\tau(L, \nu)\rangle = \frac{1}{\Delta\nu} \int_{\Delta\nu} \exp\left[-K(\nu)u\right]d\nu. \tag{4}$$

The average absorption A over the interval $\Delta\nu$ is then

$$A = \frac{1}{\Delta\nu} \int_{\Delta\nu}\left\{1 - \exp\left[-K(\nu)u\right]\right\}d\nu. \tag{5}$$

Finally, we denote the equivalent line width by $W = A\Delta\nu$.

$$W = \int_{\Delta\nu}\left\{1 - \exp\left[-K(\nu)u\right]\right\}d\nu. \tag{6}$$

The absorption coefficient for gases is a strong function of frequency. This dependence is formulated in terms of line shapes: Lorentz, Doppler, Lorentz-Doppler, etc. Various causes contribute to the widths of spectral lines, two of the main factors being Doppler width and pressure broadening. The Doppler width results from the thermal motion of the species, whereas pressure broadening is due to collision bombardment which is dependent on temperature, density, and overall composition of the gaseous mixture containing the emitting atoms. Thus, a gaseous system containing many colliding molecules gives rise to what are called Lorentz pressure broadened lines. Various models, therefore, exist which are based on particular spectral line shapes, location, intensity, half-width, and their dependence of pressure and temperature.

Self-reversal also occurs when the radiation passes through its own vapor and is partially absorbed. In general, the center of the line or band is preferentially absorbed relative to the wings. This causes a decrease in the central maximum and a corresponding increase in the defined line width. This reversal width depends on gas pressure and temperature and is highly dependent on path length. If complete reversal occurs, then a given line will appear to be a spurious doublet since the center is completely absorbed.

Lines broadened by collisions have a collision or Lorentz half-width (a_L) which is a function of both pressure and temperature.

$$a_L = a_0 \left(\frac{P}{P_0}\right)\left(\frac{T_0}{T}\right)^{\frac{1}{2}} \text{cm}^{-1}, \tag{7}$$

where a_0 is the half-width at the conditions of P_0, T_0. In this expression, the equivalent pressure of the gaseous mixture P_e should be used since the absorbing molecules are a more effective broadening agent than other molecules, which may be present. However, for small concentrations or partial pressures of CO_2, the total pressure can be assumed equal to the equivalent pressure.

The Doppler half-width (a_D) is given by the expression

$$a_D = \nu_0 \sqrt{\frac{T}{M}} \left\{\frac{2KN_A \ell n 2}{C^2}\right\}^{\frac{1}{2}} \text{cm}^{-1}, \tag{8}$$

where ν_0 is the line center, T is the absolute temperature, and M is the molecular weight of the molecule. The quantities K, N_A, and C are the Boltzmann and Avagadro constants and the speed of light, respectively. Inserting the numerical value of these constants into the

above expression in brackets, we obtain

$$a_D = 3.583 \times 10^{-7} \nu_0 \sqrt{\frac{T}{M}} . \tag{8a}$$

For the 4.3-micron CO_2 band, $\nu_0 = 2350\ cm^{-1}$ and M = 44.

$$a_D = 1.269 \times 10^{-4} \sqrt{T}\ cm^{-1}. \tag{8b}$$

At a pressure of 1 atm and a temperature of 300°K, the Lorentz half-width is $1.3\ cm^{-1}$. For small concentrations of CO_2, Equation (7) may be written as

$$a_L = 1.3 \frac{P}{T^{\frac{1}{2}}}\ cm^{-1}, \tag{9}$$

where P is the total pressure of the gaseous mixture containing CO_2. A comparison of the Doppler and Lorentz line widths can now be obtained by considering the ratio

$$a_L/a_D = 1.3\ PT^{-\frac{1}{2}}/1.269 \times 10^{-4} T^{\frac{1}{2}} \simeq 10^4 \frac{P}{T}. \tag{10}$$

At normal atmospheric pressure and the temperature range considered in this report, it is seen that the Lorentz broadening dominates. For the Lorentz line shape, the absorption coefficient is given by the expression (Ref. 3)

$$K(\nu) = \frac{S}{\pi} \frac{a_L}{(\nu - \nu_0)^2 + (a_L)^2}, \tag{11}$$

where S is the intensity of the line located at the wavenumber ν_0 whose half-width is a_L. If this half-width is now denoted simply by a, Equation (6) can be written as

$$W = \int_{\Delta\nu} \left\{ 1 - \exp - \left[\left(\frac{Sua}{\pi} \right) \frac{1}{(\nu - \nu_0)^2 + a^2} \right] \right\} d\nu. \tag{12}$$

The integration may now be extended over all wavenumber space by assuming there is no absorption outside the interval $\Delta\nu$. By extending the integration over all wavenumber space, the location of ν_0 has no significance and can therefore be dropped from the above expression. The integrand then becomes an even function and the

equivalent width can be written as

$$W = 2\int_0^\infty \left\{1 - \exp - \left(\frac{2a^2X}{\nu^2 + a^2}\right)\right\} d\nu, \tag{13}$$

where $X = Su/2\pi a$. The mapping $\nu = a \cot(\Theta/2)$ can now be made which transforms the above integral into the expression

$$W = 2a\int_0^\pi \left\{1 - e^{-X(1 - \cos\Theta)}\right\} \frac{d\Theta}{1 - \cos\Theta}. \tag{14}$$

The exponent in the integrand can be expanded into a series and integrated term-by-term to give

$$W = 2\pi a X \sum_{n=0}^{\infty} \frac{(-)^n X^n \Gamma(2n + 1)}{2n(n + 1)\left\{\Gamma(n + 1)\right\}^3}. \tag{15}$$

An integration by parts can also be performed by choosing $U = 1 - \exp\left[-X(1 - \cos\Theta)\right]$, $dV = d\Theta(1 - \cos\Theta)^{-1}$. The UV term then vanishes at the limits giving

$$W = 2\pi a X e^{-X} \int_0^\pi \left[\exp(X\cos\Theta) + \cos\Theta \exp(X\cos\Theta)\right] d\Theta. \tag{16}$$

The integrand is now in a form to be readily recognized as Bessel functions (Ref. 9). Therefore,

$$W = 2\pi a X e^{-X}\left[I_0(X) + I_1(X)\right], \tag{17}$$

where $I_n(X)$ is a modified Bessel function which has a complex argument; i.e.,

$$I_n(X) = e^{-i\pi n/2} J_n(iX) \tag{18}$$

$$I_0(X) = J_0(iX)$$

$$I_1(X) = iJ_1(iX). \tag{19}$$

This gives the equivalent width of a single line having a Lorentz shape. This must now be extended to obtain the absorption from a band which consists of many lines.

Consider a band of width $\Delta\nu$ made up of n lines. The transmission of the ith line which is centered at ν_i is

$$\tau_i = e^{-K(\nu_i)u}. \tag{20}$$

The average transmissivity over the interval $\Delta\nu$ is obtained by averaging overall intensities and positions of the various lines. It is postulated that these quantities can be specified by probability functions. For the various lines it is assumed that $\psi(\nu_1, \nu_2, \ldots \nu_n)$ is the probability that the first line is centered in the interval $d\nu_1$, when the center of the second line is in the interval $d\nu_2, \ldots$, when the center of the nth line is in the interval $d\nu_n$. Also, $P(S_i)dS_i$ is the probability that the ith line will have an intensity S_i in the range dS_i. The average transmission can then be written as (Ref. 2)

$$\langle\tau\rangle = \frac{\int_{\Delta\nu}\cdots\int_{\Delta\nu}\psi(\nu_1,\nu_2,\ldots,\nu_n)d\nu_1 d\nu_2\ldots d\nu_n \int_0^\infty\cdots\int_0^\infty \prod_{i=1}^{n} P(S_i)e^{-K(\nu_i)u}dS_i}{\int_{\Delta\nu}\cdots\int_{\Delta\nu}\psi(\nu_1,\nu_2,\ldots,\nu_n)d\nu_1 d\nu_2\ldots d\nu_n \int_0^\infty\cdots\int_0^\infty \prod_{i=1}^{n} P(S_i)dS_i}. \tag{21}$$

Since the probability of finding a given line with intensity S_i must be unity if the entire intensity space is spanned, then $P(S_i)$ must be capable of being normalized if it is to be an acceptable probability function; i.e.,

$$\int_0^\infty P(S_i)dS_i = 1. \tag{22}$$

Also, it will be assumed that ψ is a constant. This implies equal probability for each line being centered at a given spectral location in the band whatever the location of the other lines. The average transmissivity can then be written as

$$\langle\tau\rangle = \frac{1}{(\Delta\nu)^n}\int_{\Delta\nu}\cdots\int_{\Delta\nu} d\nu_1\cdots d\nu_n \int_0^\infty\cdots\int_0^\infty \prod_i P(S_i)e^{-K(\nu_i)u}dS_i. \tag{23}$$

The n lines comprising the band $\Delta\nu$ are now assumed to have an average spacing d such that $nd = \Delta\nu$. Since all of the n integrals above are equal, then

$$\langle\tau\rangle = \left\{\frac{1}{nd}\int_{\Delta\nu}\left[\int_0^\infty P(S)e^{-K(\nu)u}dS\right]d\nu\right\}^n. \tag{24}$$

or

$$\langle\tau\rangle = \left\{1 - \frac{1}{nd}\int_{\Delta\nu}\left[\int_0^\infty P(S)\left(1 - e^{-K(\nu)u}\right)dS\right]d\nu\right\}^n. \tag{25}$$

Using Equation (6), this may be written as

$$\langle\tau\rangle = \left\{1 - \frac{1}{nd}\int_0^\infty W(S)P(S)dS\right\}^n, \tag{26}$$

where W is the equivalent width for a single line. For the distribution of line strengths P(S), the average equivalent width is

$$\langle W\rangle = \int_0^\infty W(S)P(S)dS. \tag{27}$$

Utilizing this expression for the average equivalent width and letting the value of n increase without limit in Equation (26) while constraining d to remain constant, we obtain

$$\langle\tau\rangle = 1 - \langle A\rangle = \exp - (\langle W\rangle/d). \tag{28}$$

Finally, we take the average absorption equal to the emissivity and make use of the equivalent width in Equation (17) to obtain the expression

$$\epsilon = 1 - \exp - \left\{\frac{2\pi a X e^{-X}}{d}\left[I_0(X) + I_1(X)\right]\right\}. \tag{29}$$

This describes the band emission assuming a statistical model of the band with an infinite number of lines having a Lorentz shape.

Let us now consider the function (known as the Ladenburg-Reiche function)

$$F(X) = Xe^{-X}\left[I_0(X) + I_1(X)\right], \tag{30}$$

which is also equivalent to Equation (15). For small values of X, this function can be written

$$F(X) \sim X\left(1 - \frac{X}{2} + \frac{X^2}{4} - \ldots\right) \simeq X. \tag{31}$$

For large values of X, an asymptotic expansion gives (Ref. 10)

$$F(X) \sim \sqrt{\frac{2X}{\pi}}\left\{1 - \frac{1}{8X} - \frac{3}{128X^2}\right\} \simeq \sqrt{\frac{2X}{\pi}}\,. \tag{32}$$

Preliminary investigations utilizing Equation (29) showed that the emissivity was overestimated using this growth function and available band parameters. Also, for computational efficiency it is desirable to use a simplier algebraic expression so as to avoid the rather cumbersome Bessel functions. The success of Ref. 6 at temperatures above 1000°K then prompted the adoption of the function

$$F(X) = \frac{1}{\pi}\left\{(1 + 2\pi X)^{\frac{1}{2}} - 1\right\}, \tag{33}$$

as suggested by M[illegible]cmus (Ref. 11). For small X this reduces to

$$F(X) \simeq \frac{1}{\pi}\{2\pi X\} = X, \tag{31}$$

and for large X

$$F(X) = \frac{1}{\pi}\left\{\sqrt{2\pi X}\left(1 + \frac{1}{2\pi X}\right)^{\frac{1}{2}} - 1\right\} \simeq \frac{1}{\pi}\sqrt{2\pi X}\left\{\frac{1}{4\pi X} + 1\right\} \simeq \sqrt{\frac{2X}{\pi}}. \tag{32}$$

This function, Equation (33), grows less rapidly than the Ladenburg-Reiche curve (see Figure 1). However, it produces good agreement between calculated emissivities and experimentally determined values, significantly reduces calculation times required for numerical work, and, at the asymptotic limits, reduces to the weak and strong line extremes; i. e.,

$$\lim_{X \to 0} F(X) = X,$$

$$\lim_{X \to \infty} F(X) = \sqrt{\frac{2X}{\pi}}$$

We can now summarize at this point by writing the equation chosen to represent the model for the spectral emissivity calculations of a homogeneous medium.

$$\epsilon = 1 - \exp\left\{\frac{-2\alpha P_T}{d}\left[\left(1 + \frac{SP_{CO_2}L}{P_T\alpha}\right)^{\frac{1}{2}} - 1\right]\right\}, \qquad (34)$$

where

$$\alpha \propto T^{-\frac{1}{2}},$$

$$d = d(\nu, T),$$

$$S = S(\nu, T).$$

Before considering any inhomogenous calculations, we will, for continuity, carry the homogeneous discussion completely through. At this point it is now necessary to consider the band parameters S and d.

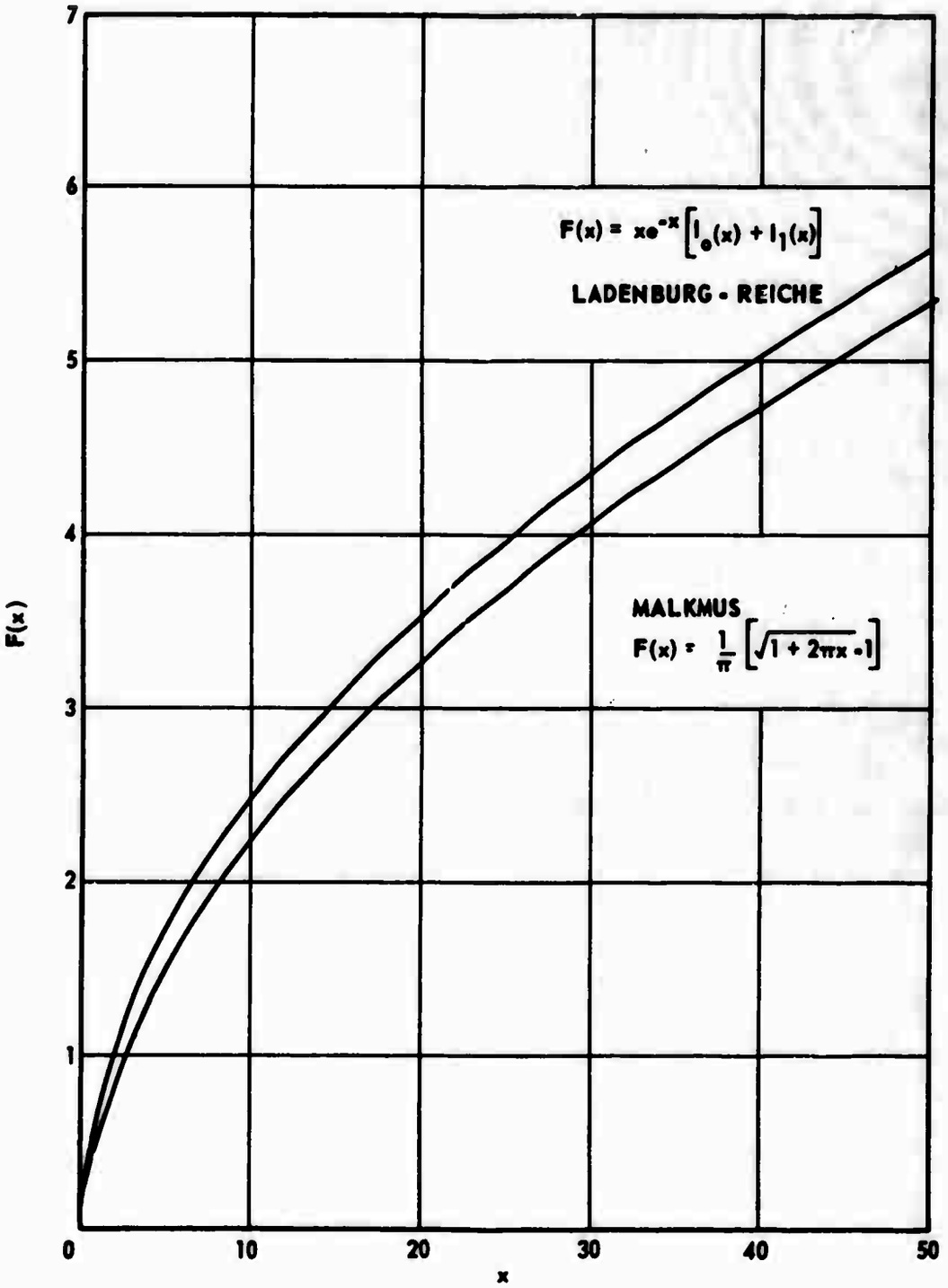

Figure 1. Comparison of Ladenburg-Reiche and Malkmus Growth Functions

Section IV. BAND PARAMETERS

The carbon dioxide molecule has received a great deal of study, both theoretical and experimental; much of which has been done at relatively low temperatures because of interest in atmospheric absorption or transmission problems. A limited amount of information exists for the 4.3-micron band over portions of the temperature range of interest (300°to 2100°K) chosen for this study. Since the theoretical calculation of the band parameters is rather complicated, values of the average integrated intensity of a rotational line, as well as the average distance between the spectral lines, were obtained or derived from existing literature data. Where gaps and regions of overlapping disagreement existed, interpolation, extrapolation, a best curve fit, or comparison with available experimental data results was used for continuity.

A careful study of available data at 300°K showed that no satisfactory band parameters were available which could be used for the selected model. However, transmission tables at the desired temperature were available over a wide range of path lengths and pressures (Ref. 7). These tables were constructed from the quasirandom model, which is the most accurate band model available. The calculation included the contribution from all isotopic species having an intensity greater than 10^{-3} of the strongest line in a particular spectral region. Results were presented every 5 cm^{-1} along with averaged values over 20, 50, and 100 cm^{-1}. The data that were averaged over 20 cm^{-1} were used for this report. The band parameters were derived by making a least squares fit of the data to the statistical model. It should again be noted, as was pointed out in Section I, that these parameters are very dependent on the model chosen to represent the spectral emissivity. Since the statistical model has been adopted, we can write,

$$\epsilon = 1 - \exp - \left\{ \frac{2\alpha P_T}{d} \left[\sqrt{1 + \frac{SL_e}{\alpha}} - 1 \right] \right\} . \tag{35}$$

If the transmissivity is denoted as $\tau = 1 - \epsilon$, then for a total pressure of 1 atm the previous equation can be rearranged to read

$$\frac{1}{4\alpha(S\frac{1}{2}/d)^2} \ln(1/\tau) + \frac{1}{S/d} = \frac{L_e}{\ln(1/\tau)} , \tag{36}$$

which is of the form

$$Y = aX + b, \tag{37}$$

with

$$Y = L_e/\ell n(1/\tau)$$

$$a = (S/d)^{-1}$$

$$X = \ell n(1/\tau)$$

$$b = (S\tfrac{1}{2}/d)^{-2}/4a.$$

This is now a linear equation which easily admits to a least squares fit. The slope of the line and its intercept define the desired band parameters. The data of Stull, Wyatt, and Plass (Ref. 7) were then fitted to the above equation to give the band parameters at 300°K. The mathematical procedure was to solve the following pair of simultaneous equations:

$$\sum_{i=1}^{n} \frac{(L_e)_i}{\ell n \tau_i} = -\frac{n}{(S/d)} + \frac{1}{4a\,(S\tfrac{1}{2}/d)^2}\,\ell n\left\{\prod_{i=1}^{n} \tau_i\right\}, \tag{38}$$

$$\sum_{i=1}^{n} (L_e)_i = -\frac{1}{(S/d)}\,\ell n\left\{\prod_{i=1}^{n} \tau_i\right\} + \frac{1}{4a(S\tfrac{1}{2}/d)^2} \sum_{i=1}^{n} (\ell n \tau_i)^2, \tag{39}$$

where n is the number of points being considered.

At 600°K, data from three sources—Plass (Ref. 12), Gray (Ref. 5), and Malkmus (Ref. 8)—were available for the ratio of the parameters S/d. The average values of these data were used. For the ratio of the parameters $S\tfrac{1}{2}/d$, data at 600°K were available from Gray and Malkmus. Again the average values were used for this program. At the higher temperatures (1200° to 2100°K), data for these two parameters have been computed by both Ben-Aryeh (Ref. 6) and Malkmus with the result of the latter being extended to lower wavenumbers. In the vicinity of 2200 cm^{-1} there was some disagreement between the $S\tfrac{1}{2}/d$ results. Average values were again used to obtain the band parameters in this region. At shorter wavelengths the agreement was good, and the calculations of Ben-Aryeh were utilized since his results were tabulated.

Since it was desirable to have tabulated data at least every 300°K, values of the band parameters were then obtained at 900°K by interpolation. The method utilized was to plot the band parameter of interest as a function of temperature for a particular spectral point and then determine the value of the parameter at the desired temperature. Next a plot cross-plot technique was used to extrapolate values for existing gaps of the data matrix to complete the range ($300 \leq T \leq 2100$°K and $2050 \leq \nu \leq 2400$ cm^{-1}). A six-point Lagrangian interpolation scheme, in essence of fifth degree polynomial in wavelength at constant temperature, was then used to refine any remaining data to the desired 5-cm^{-1} spectral resolution to be used in the final program.

Typical results are shown in Figures 2 through 5. Also, the band parameters are listed in Tables I and II.

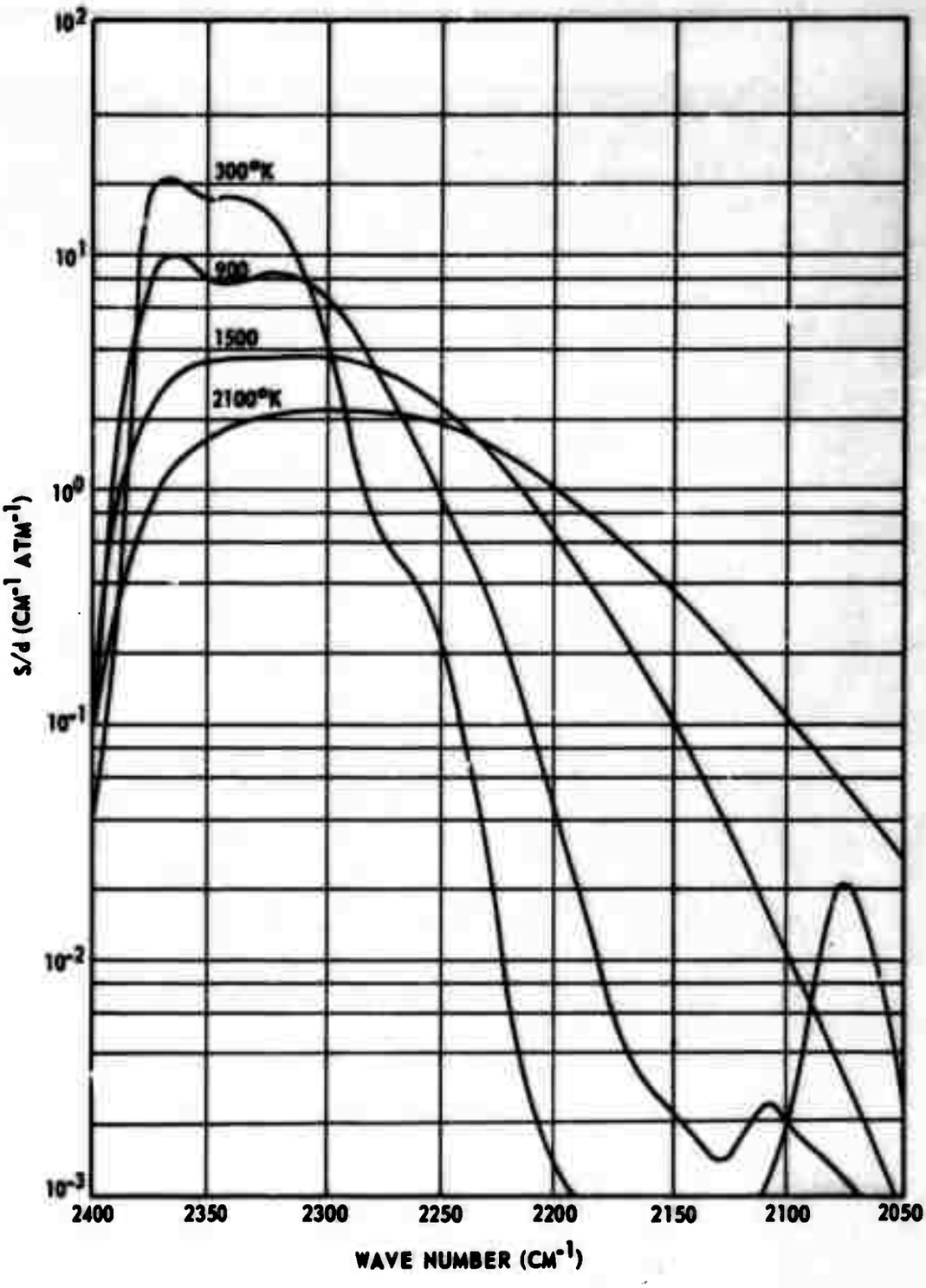

Figure 2. S/d Versus Wavenumber with Temperature as a Parameter

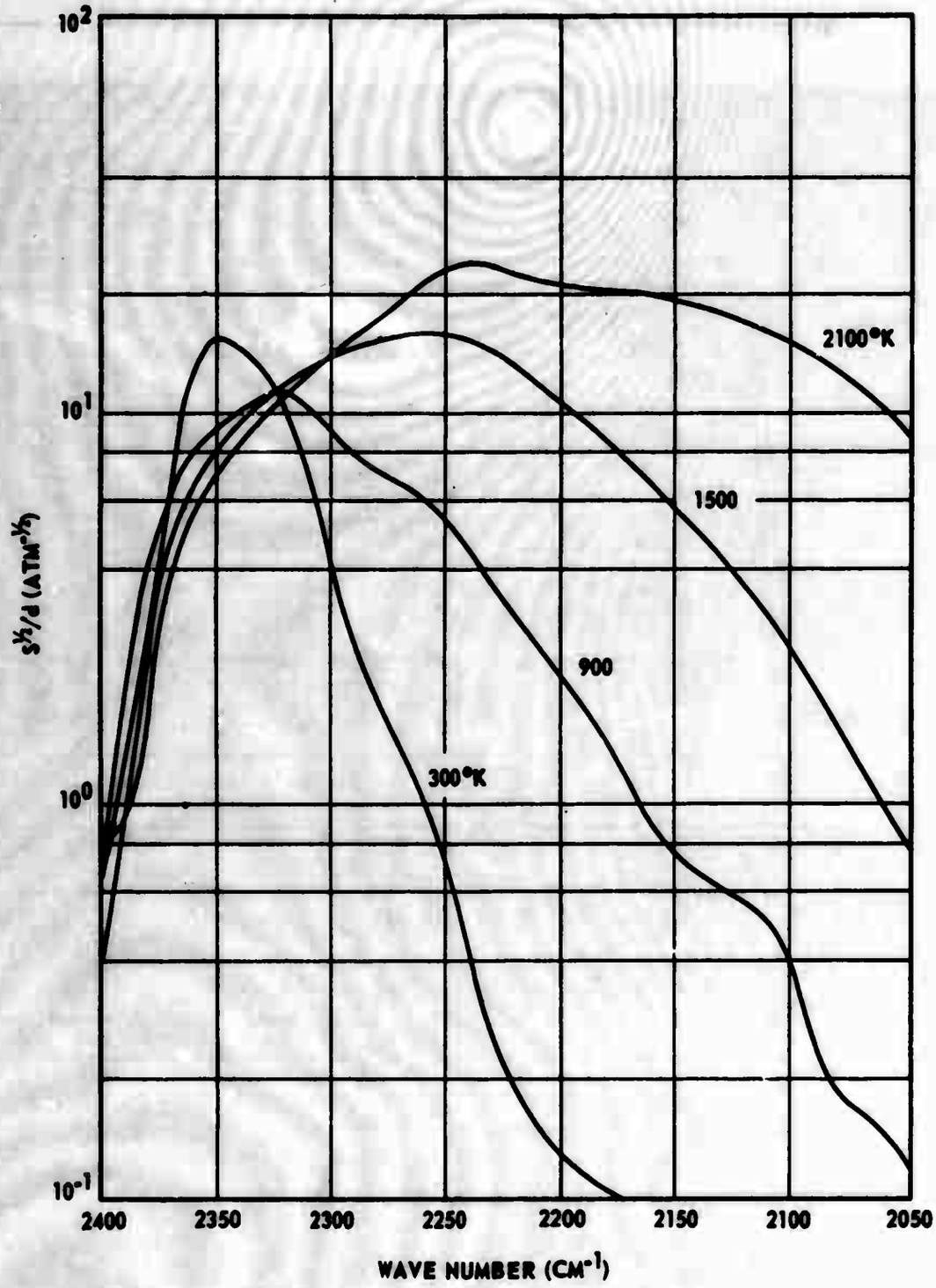

Figure 3. $S^{1/2}/d$ Versus Wavenumber with Temperature as a Parameter

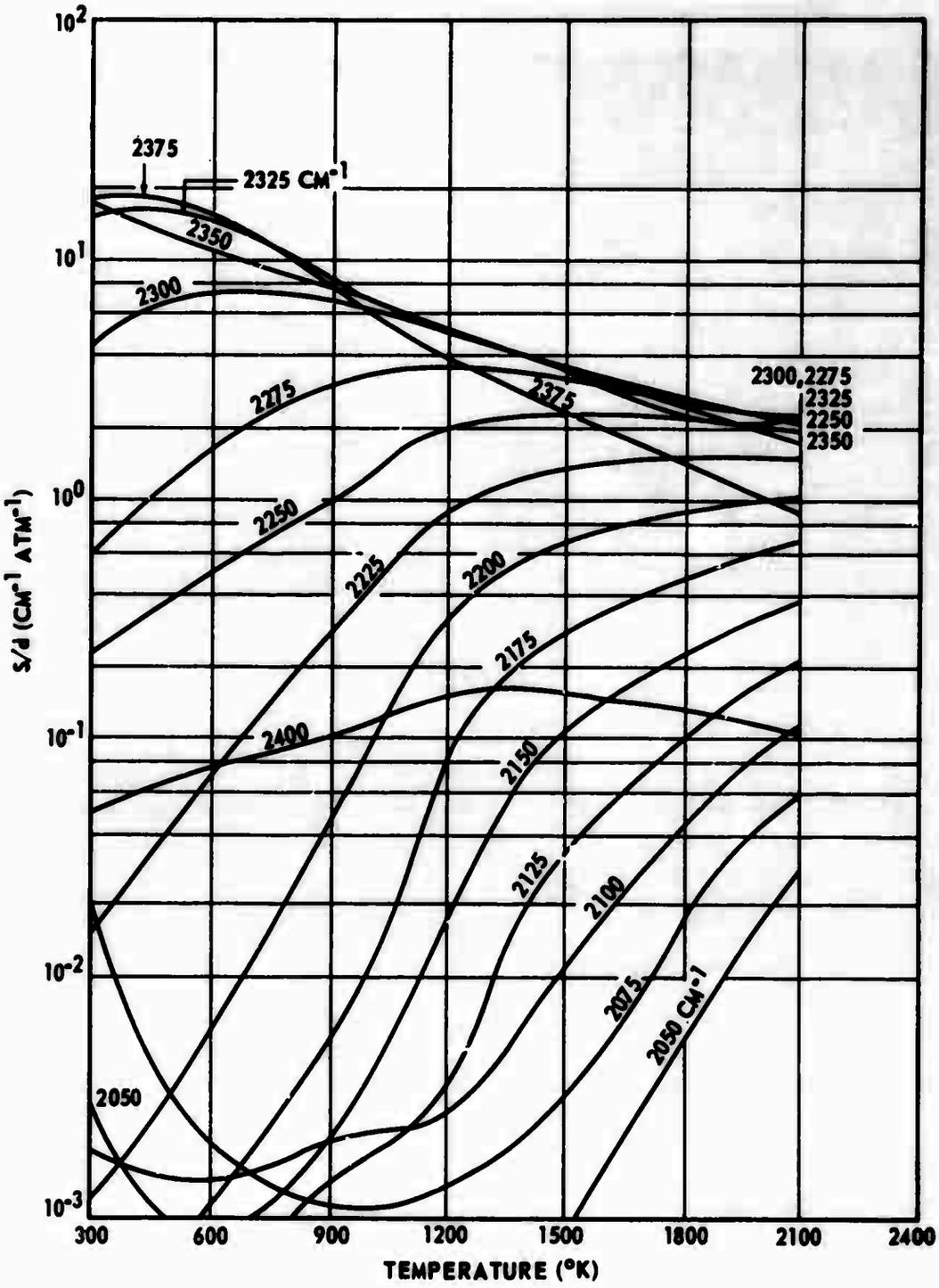

Figure 4. S/d Versus Temperature with Wavenumber as a Parameter

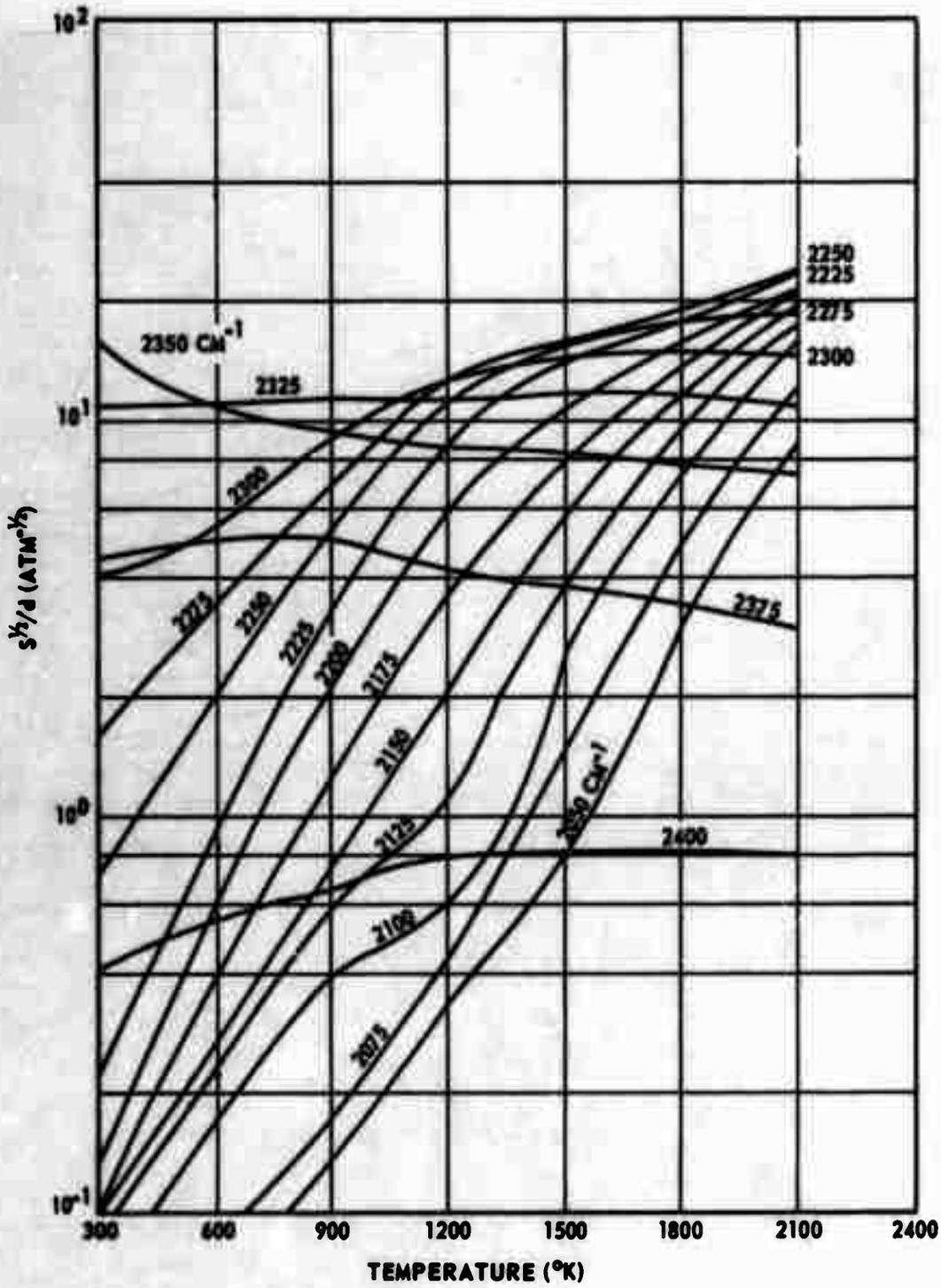

Figure 5. $S^{1/2}/d$ Versus Temperature with Wavenumber as a Parameter

Table I. The Spectral Band Parameter S/d as a Function of Temperature

WAVE NUMBER (1/CM)	TEMPERATURE (DEGREES KELVIN) 300.	600.	900.	1200.	1500.	1800.	2100.
2050.	2.60E-03	4.80E-04	3.40E-04	4.10E-04	8.20E-04	5.70E-03	2.60E-02
2055.	4.80E-03	7.00E-04	4.50E-04	5.20E-04	1.08E-03	7.20E-03	3.00E-02
2060.	9.01E-03	1.03E-03	5.72E-04	6.37E-04	1.37E-03	9.08E-03	3.56E-02
2065.	1.40E-02	1.51E-03	7.53E-04	8.23E-04	1.77E-03	1.14E-02	4.12E-02
2070.	1.87E-02	1.89E-03	9.57E-04	1.06E-03	2.28E-03	1.42E-02	4.76E-02
2075.	2.02E-02	2.08E-03	1.15E-03	1.34E-03	2.95E-03	1.75E-02	5.47E-02
2080.	1.65E-02	1.99E-03	1.30E-03	1.66E-03	3.81E-03	2.13E-02	6.28E-02
2085.	1.08E-02	1.79E-03	1.44E-03	2.04E-03	4.96E-03	2.58E-02	7.21E-02
2090.	6.31E-03	1.63E-03	1.57E-03	2.54E-03	6.41E-03	3.08E-02	8.30E-02
2095.	3.21E-03	1.52E-03	1.77E-03	2.81E-03	8.23E-03	3.65E-02	9.51E-02
2100.	1.81E-03	1.47E-03	2.10E-03	2.65E-03	1.06E-02	4.28E-02	1.08E-01
2105.	1.33E-03	1.41E-03	2.35E-03	2.30E-03	1.36E-02	5.01E-02	1.24E-01
2110.	9.55E-04	1.26E-03	2.32E-03	1.89E-03	1.73E-02	5.86E-02	1.41E-01
2115.	6.95E-04	1.07E-03	2.08E-03	1.86E-03	2.21E-02	6.86E-02	1.60E-01
2120.	5.65E-04	8.82E-04	1.70E-03	2.46E-03	2.80E-02	8.05E-02	1.81E-01
2125.	5.13E-04	7.36E-04	1.40E-03	3.52E-03	3.51E-02	9.61E-02	2.05E-01
2130.	4.88E-04	6.96E-04	1.38E-03	4.98E-03	4.38E-02	1.15E-01	2.31E-01
2135.	4.80E-04	7.11E-04	1.53E-03	6.91E-03	5.46E-02	1.37E-01	2.61E-01
2140.	4.78E-04	7.30E-04	1.73E-03	9.55E-03	6.73E-02	1.63E-01	2.95E-01
2145.	4.82E-04	7.52E-04	1.95E-03	1.31E-02	8.27E-02	1.92E-01	3.32E-01
2150.	4.91E-04	7.81E-04	2.20E-03	1.82E-02	1.01E-01	2.25E-01	3.73E-01
2155.	5.05E-04	8.16E-04	2.47E-03	2.52E-02	1.24E-01	2.62E-01	4.18E-01
2160.	5.22E-04	8.56E-04	2.78E-03	3.43E-02	1.53E-01	3.06E-01	4.68E-01
2165.	5.47E-04	9.16E-04	3.25E-03	4.63E-02	1.88E-01	3.55E-01	5.22E-01
2170.	5.81E-04	1.01E-03	4.03E-03	6.16E-02	2.28E-01	4.07E-01	5.80E-01
2175.	6.28E-04	1.18E-03	5.68E-03	8.20E-02	2.76E-01	4.67E-01	6.42E-01
2180.	6.95E-04	1.46E-03	8.82E-03	1.09E-01	3.32E-01	5.36E-01	7.10E-01
2185.	7.83E-04	1.91E-03	1.40E-02	1.43E-01	3.95E-01	6.13E-01	7.82E-01
2190.	9.01E-04	2.60E-03	2.18E-02	1.88E-01	4.70E-01	7.00E-01	8.57E-01
2195.	1.06E-03	3.91E-03	3.34E-02	2.46E-01	5.58E-01	7.93E-01	9.32E-01
2200.	1.28E-03	6.27E-03	5.00E-02	3.15E-01	6.56E-01	8.93E-01	1.00E-00
2205.	1.69E-03	1.02E-02	7.20E-02	3.97E-01	7.67E-01	1.00E-00	1.08E-00
2210.	2.45E-03	1.65E-02	1.00E-01	4.92E-01	8.88E-01	1.11E-00	1.17E-00
2215.	4.28E-03	2.74E-02	1.41E-01	6.01E-01	1.01E-00	1.23E-00	1.26E-00
2220.	7.95E-03	4.54E-02	2.02E-01	7.28E-01	1.16E-00	1.35E-00	1.36E-00

Table I (concluded)

WAVE NUMBER (1/CM)	TEMPERATURE (DEGREES KELVIN) 300.	600.	900.	1200.	1500.	1800.	2100.
2225.	1.60E-02	7.54E-02	2.79E-01	8.76E-01	1.31E-00	1.48E-00	1.45E-00
2230.	3.10E-02	1.22E-01	3.67E-01	1.04E-00	1.48E-00	1.61E-00	1.55E-00
2235.	5.71E-02	1.85E-01	4.73E-01	1.24E-00	1.65E-00	1.74E-00	1.64E-00
2240.	9.84E-02	2.66E-01	6.0?E-01	1.46E-00	1.84E-00	1.86E-00	1.72E-00
2245.	1.56E-01	3.65E-01	7.70E-01	1.71E-00	2.03E-00	1.99E-00	1.80E-00
2250.	2.32E-01	4.86E-01	9.75E-01	1.98E-00	2.22E-00	2.11E-00	1.87E-00
2255.	3.15E-01	6.30E-01	1.22E-00	2.28E-00	2.42E-00	2.22E-00	1.93E-00
2260.	3.93E-01	7.98E-01	1.53E-00	2.60E-00	2.61E-00	2.32E-00	1.98E-00
2265.	4.63E-01	1.00E-00	1.90E-00	2.93E-00	2.79E-00	2.41E-00	2.03E-00
2270.	5.21E-01	1.26E-00	2.36E-00	3.27E-00	2.96E-00	2.49E-00	2.06E-00
2275.	6.17E-01	1.63E-00	2.89E-00	3.61E-00	3.12E-00	2.55E-00	2.08E-00
2280.	7.99E-01	2.20E-00	3.52E-00	3.94E-00	3.26E-00	2.61E-00	2.10E-00
2285.	1.17E-00	3.05E-00	4.25E-00	4.25E-00	3.38E-00	2.65E-00	2.11E-00
2290.	1.84E-00	4.32E-00	5.10E-00	4.53E-00	3.48E-00	2.69E-00	2.12E-00
2295.	2.89E-00	5.83E-00	5.96E-00	4.76E-00	3.55E-00	2.70E-00	2.12E-00
2300.	4.40E-00	7.42E-00	6.77E-00	4.95E-00	3.60E-00	2.71E-00	2.11E-00
2305.	6.36E-00	9.18E-00	7.44E-00	5.07E-00	3.62E-00	2.70E-00	2.10E-00
2310.	8.72E-00	1.12E+01	7.90E-00	5.14E-00	3.63E-00	2.69E-00	2.07E-00
2315.	1.11E+01	1.31E+01	8.16E-00	5.16E-00	3.62E-00	2.67E-00	2.05E-00
2320.	1.34E+01	1.46E+01	8.25E-00	5.14E-00	3.60E-00	2.65E-00	2.01E-00
2325.	1.53E+01	1.51E+01	8.18E-00	5.12E-00	3.59E-00	2.64E-00	1.99E-00
2330.	1.67E+01	1.42E+01	7.97E-00	5.08E-00	3.57E-00	2.61E-00	1.95E-00
2335.	1.75E+01	1.27E+01	7.70E-00	5.08E-00	3.56E-00	2.57E-00	1.90E-00
2340.	1.76E+01	1.11E+01	7.45E-00	5.10E-00	3.55E-00	2.53E-00	1.85E-00
2345.	1.74E+01	1.03E+01	7.43E-00	5.15E-00	3.52E-00	2.46E-00	1.76E-00
2350.	1.73E+01	1.11E+01	7.87E-00	5.27E-00	3.50E-00	2.40E-00	1.69E-00
2355.	1.81E+01	1.32E+01	8.85E-00	5.35E-00	3.43E-00	2.29E-00	1.59E-00
2360.	1.95E+01	1.56E+01	1.00E+01	5.33E-00	3.28E-00	2.12E-00	1.43E-00
2365.	2.09E+01	1.71E+01	1.01E+01	5.11E-00	3.05E-00	1.94E-00	1.29E-00
2370.	2.11E+01	1.80E+01	9.50E-00	4.90E-00	2.69E-00	1.67E-00	1.09E-00
2375.	1.82E+01	1.60E+01	7.83E-00	3.91E-00	2.28E-00	1.41E-00	8.50E-01
2380.	1.01E+01	7.20E-00	6.00E-00	3.07E-00	1.77E-00	1.05E-00	6.50E-01
2385.	1.19E-00	2.54E-00	3.45E-00	2.19E-00	1.35E-00	8.02E-01	4.50E-01
2390.	2.97E-01	9.97E-01	1.70E-00	1.20E-00	7.80E-01	4.80E-01	3.00E-01
2395.	9.75E-02	2.61E-01	3.62E-01	4.95E-01	3.81E-01	3.21E-01	1.75E-01
2400.	5.01E-02	7.50E-02	1.00E-01	1.50E-01	1.50E-01	1.30E-01	1.00E-01

Table II. The Spectral Band Parameter $S_{\frac{1}{2}}/d$ as a Function of Temperature

WAVE NUMBER (1/CM)	TEMPERATURE (DEGREES KELVIN) 300.	600.	900.	1200.	1500.	1800.	2100.
2050.	4.60E-02	6.60E-02	1.33E-01	3.35E-01	7.90E-01	2.90E-00	8.90E-00
2055.	4.90E-02	7.00E-02	1.37E-01	3.52E-01	8.85E-01	3.20E-00	9.39E-00
2060.	5.25E-02	7.50E-02	1.49E-01	3.76E-01	1.00E-00	3.60E-00	1.00E+01
2065.	5.68E-02	8.00E-02	1.59E-01	3.92E-01	1.13E-00	4.00E-00	1.07E+01
2070.	6.00E-02	8.42E-02	1.68E-01	4.10E-01	1.28E-00	4.40E-00	1.13E+01
2075.	6.31E-02	8.81E-02	1.76E-01	4.31E-01	1.45E-00	4.81E-00	1.19E+01
2080.	6.67E-02	9.25E-02	1.84E-01	4.56E-01	1.63E-00	5.23E-00	1.25E+01
2085.	7.06E-02	1.01E-01	2.06E-01	4.81E-01	1.84E-00	5.66E-00	1.31E+01
2090.	7.42E-02	1.19E-01	2.56E-01	5.09E-01	2.06E-00	6.10E-00	1.37E+01
2095.	7.71E-02	1.42E-01	3.23E-01	5.47E-01	2.30E-00	6.55E-00	1.42E+01
2100.	7.89E-02	1.67E-01	3.95E-01	6.00E-01	2.54E-00	7.00E-00	1.47E+01
2105.	8.01E-02	1.87E-01	4.58E-01	6.71E-01	2.78E-00	7.45E-00	1.52E+01
2110.	8.13E-02	2.01E-01	5.00E-01	7.60E-01	3.04E-00	7.90E-00	1.57E+01
2115.	8.25E-02	2.10E-01	5.29E-01	8.62E-01	3.30E-00	8.33E-00	1.62E+01
2120.	8.40E-02	2.19E-01	5.58E-01	9.73E-01	3.59E-00	8.76E-00	1.66E+01
2125.	8.54E-02	2.27E-01	5.86E-01	1.09E-00	3.89E-00	9.18E-00	1.70E+01
2130.	8.68E-02	2.35E-01	6.12E-01	1.24E-00	4.19E-00	9.60E-00	1.75E+01
2135.	8.82E-02	2.43E-01	6.38E-01	1.41E-00	4.50E-00	1.00E+01	1.78E+01
2140.	8.97E-02	2.50E-01	6.66E-01	1.60E-00	4.85E-00	1.04E+01	1.82E+01
2145.	9.12E-02	2.58E-01	6.99E-01	1.80E-00	5.22E-00	1.08E+01	1.86E+01
2150.	9.28E-02	2.66E-01	7.40E-01	2.01E-00	5.63E-00	1.12E+01	1.90E+01
2155.	9.44E-02	2.77E-01	7.96E-01	2.25E-00	6.06E-00	1.16E+01	1.94E+01
2160.	9.60E-02	2.95E-01	8.77E-01	2.51E-00	6.48E-00	1.20E+01	1.98E+01
2165.	9.74E-02	3.21E-01	9.81E-01	2.81E-00	6.91E-00	1.25E+01	2.01E+01
2170.	9.87E-02	3.55E-01	1.11E-00	3.15E-00	7.35E-00	1.30E+01	2.03E+01
2175.	1.00E-01	3.90E-01	1.25E-00	3.51E-00	7.80E-00	1.34E+01	2.04E+01
2180.	1.02E-01	4.22E-01	1.40E-00	3.91E-00	8.26E-00	1.39E+01	2.05E+01
2185.	1.06E-01	4.54E-01	1.55E-00	4.35E-00	8.75E-00	1.43E+01	2.05E+01
2190.	1.12E-01	4.90E-01	1.72E-00	4.81E-00	9.27E-00	1.47E+01	2.06E+01
2195.	1.20E-01	5.31E-01	1.90E-00	5.30E-00	9.86E-00	1.51E+01	2.08E+01
2200.	1.29E-01	5.81E-01	2.10E-00	5.81E-00	1.05E+01	1.56E+01	2.10E+01
2205.	1.40E-01	6.37E-01	2.31E-00	6.35E-00	1.12E+01	1.60E+01	2.13E+01
2210.	1.52E-01	6.97E-01	2.54E-00	6.90E-00	1.19E+01	1.64E+01	2.17E+01
2215.	1.67E-01	7.64E-01	2.77E-00	7.46E-00	1.26E+01	1.68E+01	2.21E+01
2220.	1.87E-01	8.40E-01	3.02E-00	8.02E-00	1.33E+01	1.72E+01	2.25E+01

Table II (concluded)

WAVE NUMBER (1/CM)	TEMPERATURE (DEGREES KELVIN) 300.	600.	900.	1200.	1500.	1800.	2100.
2225.	2.17E-01	9.40E-01	3.31E-00	8.57E-00	1.40E+01	1.77E+01	2.30E+01
2230.	2.65E-01	1.08E-00	3.65E-00	9.12E-00	1.45E+01	1.81E+01	2.35E+01
2235.	3.34E-01	1.26E-00	4.03E-00	9.66E-00	1.50E+01	1.86E+01	2.39E+01
2240.	4.31E-01	1.48E-00	4.43E-00	1.01E+01	1.55E+01	1.89E+01	2.41E+01
2245.	5.51E-01	1.75E-00	4.84E-00	1.06E+01	1.58E+01	1.90E+01	2.38E+01
2250.	6.93E-01	2.04E-00	5.25E-00	1.11E+01	1.59E+01	1.89E+01	2.33E+01
2255.	8.50E-01	2.34E-00	5.63E-00	1.15E+01	1.60E+01	1.87E+01	2.26E+01
2260.	1.01E-00	2.65E-00	5.99E-00	1.18E+01	1.59E+01	1.85E+01	2.17E+01
2265.	1.19E-00	2.93E-00	6.29E-00	1.21E+01	1.58E+01	1.82E+01	2.07E+01
2270.	.38E-00	3.20E-00	6.55E-00	1.24E+01	1.57E+01	1.78E+01	1.96E+01
2275.	1.58E-00	3.46E-00	6.79E-00	1.26E+01	1.54E+01	1.72E+01	1.83E+01
2280.	1.81E-00	3.75E-00	7.06E-00	1.27E+01	1.52E+01	1.67E+01	1.74E+01
2285.	2.12E-00	4.05E-00	7.39E-00	1.28E+01	1.50E+01	1.62E+01	1.65E+01
2290.	2.57E-00	4.37E-00	7.80E-00	1.28E+01	1.48E+01	1.58E+01	1.59E+01
2295.	3.18E-00	4.78E-00	8.30E-00	1.28E+01	1.45E+01	1.53E+01	1.53E+01
2300.	4.01E-00	5.38E-00	8.90E-00	1.27E+01	1.42E+01	1.47E+01	1.45E+01
2305.	5.04E-00	6.22E-00	9.55E-00	1.25E+01	1.37E+01	1.42E+01	1.38E+01
2310.	6.26E-00	7.39E-00	1.02E+01	1.23E+01	1.32E+01	1.34E+01	1.30E+01
2315.	7.67E-00	8.71E-00	1.07E+01	1.20E+01	1.27E+01	1.28E+01	1.24E+01
2320.	9.31E-00	1.00E+01	1.12E+01	1.16E+01	1.22E+01	1.21E+01	1.15E+01
2325.	1.09E+01	1.10E+01	1.14E+01	1.13E+01	1.16E+01	1.14E+01	1.08E+01
2330.	1.22E+01	1.14E+01	1.12E+01	1.08E+01	1.10E+01	1.07E+01	1.00E+01
2335.	1.34E+01	1.13E+01	1.08E+01	1.03E+01	1.03E+01	9.86E-00	9.13E-00
2340.	1.44E+01	1.10E+01	1.04E+01	9.85E-00	9.70E-00	9.22E-00	8.52E-00
2345.	1.53E+01	1.06E+01	9.90E-00	9.16E-00	8.88E-00	8.36E-00	7.81E-00
2350.	1.59E+01	1.06E+01	9.50E-00	8.51E-00	8.15E-00	7.61E-00	7.22E-00
2355.	1.52E+01	9.45E-00	8.65E-00	7.77E-00	7.36E-00	6.85E-00	6.50E-00
2360.	1.30E+01	8.01E+00	7.60E-00	6.87E-00	6.33E-00	5.77E-00	5.45E-00
2365.	1.03E+01	7.27E-00	7.61E-00	6.15E-00	5.56E-00	5.05E-00	4.66E-00
2370.	6.97E-00	6.43E-00	5.90E-00	5.50E-00	4.58E-00	4.12E-00	3.67E-00
2375.	4.45E-00	4.95E-00	5.01E-00	4.10E-00	3.76E-00	3.36E-00	2.97E-00
2380.	2.65E-00	3.50E-00	4.10E-00	2.80E-00	2.30E-00	1.90E-00	1.60E-00
2385.	1.51E-00	2.28E-00	3.00E-00	2.05E-00	1.70E-00	1.27E-00	1.15E-00
2390.	9.98E-01	1.40E+00	1.90E-00	1.40E-00	1.20E-00	1.00E-00	9.00E-01
2395.	6.25E-01	7.59E-01	1.20E-00	1.09E-00	9.00E-01	8.65E-01	8.40E-01
2400.	4.03E-01	5.51E-01	6.63E-01	8.00E-01	8.00E-01	8.10E-01	8.00E-01

Section V. INTERPOLATION PROCEDURE

Since the band parameters are only tabulated every 300°K, it is obviously necessary to be able to compute emissivities at temperatures other than those listed. After considerable study, an interpolation method was chosen (Ref. 7) which is based on emissivity rather than the band parameter. Equation (34) can be written as

$$\epsilon(T) = 1 - \exp\left[G(T)\right], \tag{40}$$

when temperature is the only variable. G(T) is the functional relationship which describes the temperature variation of the argument of the exponent. This may now be rewritten as

$$G(T) = \ln\left[1 - \epsilon(T)\right]. \tag{41}$$

Now we take

$$G(T + \Delta T) = G(T) + \Delta G, \tag{42}$$

with

$$\Delta G = \frac{\partial G}{\partial T}\Delta T,$$

giving

$$G(T + \Delta T) = G(T) + \frac{\partial G}{\partial T}\Delta T. \tag{43}$$

This is simply the first two terms of the Taylor expansion. Next, let us take

$$\epsilon(T + \Delta T) = 1 - \exp\left[G(T) + \Delta G\right]. \tag{44}$$

We now assume ΔT to be positive so that the desired temperature $T_x = T_1 + \Delta T$; i.e., T_1 is the value of T occurring in the temperature data array for which $0 < T_x - T_1 < 300°K$. Finally, we take $T_2 = T_1 + 300°K$, the next tabulated data point, so that $T_1 < T_x < T_2$. Equation (43) then gives the relationship

$$G(T_x) = G(T_1) + \frac{G(T_2) - G(T_1)}{(T_2 - T_1)}(T_x - T_1), \tag{45}$$

and

$$\epsilon(T_x) = 1 - \exp G(T_x). \tag{46}$$

In order to illustrate the above, let us consider a specific example: Take P_T = 1 atm, P_{CO_2} = 0.1 atm, L = 1.0 cm, T = 1000°K, ν = 2300 cm^{-1}. Then T_1 = 900°K, T_2 = 1200°K. Using previously defined equations we now tabulate the following:

	900°K	1200°K
S/d	6.77	4.95
$S_{\frac{1}{2}}/d$	8.90	12.7
S	0.579	0.152
d	0.0855	0.0307
Y	0.0433	0.0375
X	0.213	0.0645
S/d	3.18	7.67
F(X)	0.168	0.059
G(T)	-0.536	-0.453
ϵ(T)	0.415	0.364

From Equation (45)

$$G(1000°K) = -0.536 + \left\{\frac{-0.453 + 0.536}{300}\right\}100,$$

$$G(1000°K) = -0.536 + 0.028 = -0.508,$$

and from Equation (46)

$$\epsilon(1000°K) = 0.398.$$

Section VI. COMPUTER PROGRAM

A copy of the computer program (Table III) for the homogeneous emissivity calculations is included for completeness. The program is rather unsophisticated* in that it was written for an IBM 1620 machine with limited storage capacity (the machine was conveniently located and easily accessible). In particular, the data matrix of band parameters must be read into the machine for each run because of the inability to store these quantities. The resulting emissivities are obtained on punched cards and then printed since a typed output format is rather slow. The basic program does nothing more than solve the system of equations previously described. Values of S/d and S½/d are alternately read into the computer with each set of data identified by a specific wavenumber. The spectral location, in terms of wavenumber, is also internally generated by the computer since the data are evenly spaced every 5 cm^{-1} . Thus, the computer automatically checks the input data to insure that the cards are in proper order. The other data needed by the program are the temperature (T), gas thickness (XL), total pressure (PT), and the CO_2 partial pressure (PCO2). These values are entered on a single card along with one other card which is used to document the date of the run. A typical set of input data is shown in Table IV, followed by the calculated results (Table V). One additional comment to make concerning the program is about the internal checks made on the data. The program will not accept a temperature outside the range ($300 \leq T \leq 2100°K$). A value outside this range will cause the machine to pause, type the message "TEMP OUT OF RANGE OF PROGRAM" and then branch to the beginning of the program to accept new data. Similarly, if the data cards for the band parameters are not in order, the machine gives the message "DATA CARD OUT OF SEQUENCE" and again, after pausing, returns to the beginning of the program.

* The author has also programmed the inhomogeneous calculations for a larger computer (IBM 7094) which combines a flow field program with the emission model so that plume radiation calculations may be performed. A description of this program is presently being prepared for publication.

Table III. CO_2 Emissivity Program

```
C     CO2 EMISSIVITY PROGRAM
      DIMENSION X(7),Y(7),TT(7),A(2),B(2),ARG(2),EM(72),C1(2),C2(2)
C*****************************************************************
C
C     SET UP TEMPERATURE ARRAY TO IDENTIFY THE BAND PARAMETERS
C
      DO 1 I=1,7
    1 TT(I)=300*I
C*****************************************************************
C
C     READ DATE OF RUN
C
      READ 101
  101 FORMAT(10H          )
C*****************************************************************
C
C     READ INPUT DATA
C     T=TEMPERATURE(DEGREES KELVIN)
C     XL=GAS THICKNESS(CM)
C     PT=TOTAL PRESSURE(ATM)
C     PCO2=CO2 PARTIAL PRESSURE(ATM)
C
    2 READ 100,T,XL,PT,PCO2
  100 FORMAT(4E10.4)
C*****************************************************************
C
C     PUNCH OUTPUT HEADINGS
C
      PUNCH 101
      PUNCH 102
  102 FORMAT(20H CO2 EMISSIVITY DATA)
      PUNCH 103
  103 FORMAT(1H )
C*****************************************************************
C
C     CHECK TO INSURE TEMPERATURE IS WITHIN ALLOWABLE LIMITS
C
      IF(T-300.)3,4,4
    3 PRINT 104
  104 FORMAT(29H TEMP OUT OF RANGE OF PROGRAM)
      PAUSE
      GO TO 2
    4 IF(T-2100.)5,5,3
C*****************************************************************
C
C     SEARCH TEMPERATURE ARRAY TO LOCATE THE UPPER VALUE TO BE USED IN
C     THE INTERPOLATION SCHEME
C
    5 DO 6 I=1,7
      K=I
      IF(TT(I)-T)6,6,7
    6 CONTINUE
    7 PS=PCO2*XL
```

Table III (continued)

```
C*************************************************************************
C
C     PUNCH IDENTIFICATION OF THE INPUT FOR THE RUN
C
      PUNCH 105,T
  105 FORMAT(13H TEMPERATURE=,F7.1)
      PUNCH 106,PT
  106 FORMAT(16H TOTAL PRESSURE=,E10.4)
      PUNCH 107,PS
  107 FORMAT(26H CO2 PRESSURE X THICKNESS=,E10.4)
      PUNCH 103
C*************************************************************************
C
C     READ WAVELENGTH AND BAND PARAMETERS
C
      DO 12 I=1,71
      READ 108,W1,X(1),X(2),X(3),X(4),X(5),X(6),X(7)
      READ 108,W2,Y(1),Y(2),Y(3),Y(4),Y(5),Y(6),Y(7)
  108 FORMAT(F7.1,7E9.2)
C*************************************************************************
C
C     CHECK TO INSURE INPUT DATA IS IN PROPER SEQUENCE
C
      W3=2050 + (I-1)*5
      IF(W1-W3)8,9,8
    8 PRINT 109
  109 FORMAT(26H DATA CARD OUT OF SEQUENCE)
      PAUSE
      GO TO 2
    9 IF(W2-W3)8,10,8
C*************************************************************************
C
C     COMPUTE EXPONENTIAL EMISSIVITY ARGUMENTS FOR THE TEMPERATURES
C     BOUNDED BY THE DESIRED TEMPERATURE
C
   10 DO 11 J=1,2
      M=K-1
      C1(J)=0.15*PT*SQRT(300./TT(M))
      C2(J)=PS*2.0/C1(J)
      A(J)=C1(J)*Y(M)*Y(M)/X(M)
      B(J)=1.+C2(J)*X(M)*X(M)/(Y(M)*Y(M))
      ARG(J)=A(J)*(SQRT(B(J))-1.)
   11 K=K+1
C*************************************************************************
C
C     INTERPOLATE TO OBTAIN THE DESIRED EMISSIVITY
C
      K=K-2
      DLARG=(ARG(2)-ARG(1))*(T-TT(K-1))/300.
      RARG= -(ARG(1)+DLARG)
   12 EM(I)=1.-EXP(RARG)
```

Table III (concluded)

```
C*************************************************************************
C
C     PUNCH HEADINGS FOR THE OUTPUT DATA
C
      PUNCH 110
  110 FORMAT(44H WAVENUMBER EMISSIVITY WAVENUMBER EMISSIVITY)
      PUNCH 103
C*************************************************************************
C
C     PUNCH OUTPUT DATA
C
      EM(72)=0.
      DO 13 I=1,36
      N1=2050+(I-1)*5
      N2=2050+(35+I)*5
   13 PUNCH 111,N1,EM(I),N2,EM(I+36)
  111 FORMAT(I8,3X,E11.5,I8,3X,E11.5)
C*************************************************************************
C
C     RETURN TO ACCEPT NEW SET OF INPUT DATA
C
      GO TO 2
      END
```

Table IV. Typical Input Data for Emissivity Program

```
6 MAR 69
.1000E+04 .1000E+01 .1000E+01 .1000E+00
2050.  2.60E-03 4.80E-04 3.40E-04 4.10E-04 8.20E-04 5.70E-03 2.60E-02
2050.  4.60E-02 6.60E-02 1.33E-01 3.35E-01 7.90E-01 2.90E-00 8.90E-00
2055.  4.80E-03 7.00E-04 4.50E-04 5.20E-04 1.08E-03 7.20E-03 3.00E-02
2055.  4.90E-02 7.00E-02 1.37E-01 3.52E-01 8.85E-01 3.20E-00 9.39E-00
2060.  8.01E-03 1.03E-03 5.72E-04 6.37E-04 1.37E-03 9.08E-03 3.86E-02
2060.  5.25E-02 7.50E-02 1.49E-01 3.76E-01 1.00E-00 3.60E-00 1.00E+01
2065.  1.40E-02 1.51E-03 7.53E-04 8.23E-04 1.77E-03 1.14E-02 4.12E-02
2065.  5.68E-02 8.00E-02 1.59E-01 3.92E-01 1.13E-00 4.00E-00 1.07E+01
2070.  1.87E-02 1.89E-03 9.57E-04 1.06E-03 2.28E-03 1.42E-02 4.76E-02
2070.  6.00E-02 8.42E-02 1.68E-01 4.10E-01 1.28E-00 4.40E-00 1.13E+01
2075.  2.02E-02 2.08E-03 1.15E-03 1.34E-03 2.95E-03 1.75E-02 5.47E-02
2075.  6.31E-02 8.81E-02 1.76E-01 4.31E-01 1.45E-00 4.81E-00 1.19E+01
2080.  1.65E-02 1.99E-03 1.30E-03 1.66E-03 3.81E-03 2.13E-02 6.28E-02
2080.  6.67E-02 9.25E-02 1.84E-01 4.56E-01 1.63E-00 5.23E-00 1.25E+01
2085.  1.08E-02 1.79E-03 1.44E-03 2.04E-03 4.96E-03 2.58E-02 7.21E-02
2085.  7.06E-02 1.01E-01 2.06E-01 4.81E-01 1.84E-00 5.66E-00 1.31E+01
2090.  6.31E-03 1.63E-03 1.57E-03 2.54E-03 6.41E-03 3.08E-02 8.30E-02
2090.  7.42E-02 1.19E-01 2.56E-01 5.09E-01 2.06E-00 6.10E-00 1.37E+01
2095.  3.21E-03 1.52E-03 1.77E-03 2.81E-03 8.23E-03 3.65E-02 9.51E-02
2095.  7.71E-02 1.42E-01 3.23E-01 5.47E-01 2.30E-00 6.55E-00 1.42E+01
2100.  1.81E-03 1.47E-03 2.10E-03 2.65E-03 1.06E-02 4.28E-02 1.08E-01
2100.  7.89E-02 1.67E-01 3.95E-01 6.00E-01 2.54E-00 7.00E-00 1.47E+01
2105.  1.33E-03 1.41E-03 2.35E-03 2.30E-03 1.36E-02 5.01E-02 1.24E-01
2105.  8.01E-02 1.87E-01 4.58E-01 6.71E-01 2.78E-00 7.45E-00 1.52E+01
2110.  9.55E-04 1.26E-03 2.32E-03 1.89E-03 1.73E-02 5.86E-02 1.41E-01
2110.  8.13E-02 2.01E-01 5.00E-01 7.60E-01 3.04E-00 7.90E-00 1.57E+01
2115.  6.95E-04 1.07E-03 2.08E-03 1.86E-03 2.21E-02 6.86E-02 1.60E-01
2115.  8.25E-02 2.10E-01 5.29E-01 8.62E-01 3.30E-00 8.33E-00 1.62E+01
.....
.....
.....
.....
.....
.....
.....
2375.  1.82E+01 1.60E+01 7.83E-00 3.91E-00 2.28E-00 1.41E-00 8.50E-01
2375.  4.45E-00 4.95E-00 5.01E-00 4.10E-00 3.76E-00 3.36E-00 2.97E-00
2380.  1.01E+01 7.20E-00 6.00E-00 3.07E-00 1.77E-00 1.05E-00 6.50E-01
2380.  2.65E-00 3.50E-00 4.10E-00 2.80E-00 2.30E-00 1.90E-00 1.60E-00
2385.  1.19E-00 2.54E-00 3.45E-00 2.19E-00 1.35E-00 8.02E-01 4.50E-01
2385.  1.51E-00 2.28E-00 3.00E-00 2.05E-00 1.70E-00 1.27E-00 1.15E-00
2390.  2.97E-01 9.97E-01 1.70E-00 1.20E-00 7.80E-01 4.80E-01 3.00E-01
2390.  9.98E-01 1.40E+00 1.90E-00 1.40E-00 1.20E-00 1.00E-00 9.00E-01
2395.  9.75E-02 2.61E-01 3.62E-01 4.95E-01 3.81E-01 3.21E-01 1.75E-01
2395.  6.25E-01 7.59E-01 1.20E-00 1.09E-00 9.00E-01 8.65E-01 8.40E-01
2400.  5.01E-02 7.50E-02 1.00E-01 1.50E-01 1.50E-01 1.30E-01 1.00E-01
2400.  4.03E-01 5.51E-01 6.63E-01 8.00E-01 8.00E-01 8.10E-01 8.00E-01
```

Table V. Typical Output Data from Emissivity Program

6 MAR 69
CO2 EMISSIVITY DATA

TEMPERATURE= 1000.0
TOTAL PRESSURE= .1000E+01
CO2 PRESSURE X THICKNESS= .1000E-00

WAVENUMBER	EMISSIVITY	WAVENUMBER	EMISSIVITY
2050	.35200E-04	2230	.57006E-01
2055	.46500E-04	2235	.69632E-01
2060	.58400E-04	2240	.84161E-01
2065	.77100E-04	2245	.10115E-00
2070	.98600E-04	2250	.12050E-00
2075	.12090E-03	2255	.14216E-00
2080	.14160E-03	2260	.16677E-00
2085	.16360E-03	2265	.19324E-00
2090	.18880E-03	2270	.22228E-00
2095	.21120E-03	2275	.25192E-00
2100	.22740E-03	2280	.28251E-00
2105	.23250E-03	2285	.31336E-00
2110	.21620E-03	2290	.34448E-00
2115	.19920E-03	2295	.37290E-00
2120	.19290E-03	2300	.39830E-00
2125	.20850E-03	2305	.41884E-00
2130	.25610E-03	2310	.43389E-00
2135	.32920E-03	2315	.44274E-00
2140	.43160E-03	2320	.44743E-00
2145	.56450E-03	2325	.44676E-00
2150	.75090E-03	2330	.43982E-00
2155	.10021E-02	2335	.43061E-00
2160	.13258E-02	2340	.42192E-00
2165	.17565E-02	2345	.41681E-00
2170	.23165E-02	2350	.42156E-00
2175	.31035E-02	2355	.42686E-00
2180	.42088E-02	2360	.42189E-00
2185	.56792E-02	2365	.41786E-00
2190	.76830E-02	2370	.37236E-00
2195	.10360E-01	2375	.31839E-00
2200	.13716E-01	2380	.25899E-00
2205	.17834E-01	2385	.18220E-00
2210	.22742E-01	2390	.10750E-00
2215	.28907E-01	2395	.36981E-01
2220	.36869E-01	2400	.11403E-01
2225	.46411E-01	2405	.00000E-99

Section VII. RESULTS

The ultimate test of any theoretical model is its agreement with reliable experimental data. Figures 6 and 7 show the results of the present program compared with the data of Stull, Wyatt, and Plass (Ref. 7) at a temperature of 300°K and a total pressure of 1 atm.

Figure 8 shows some of the experimental results of Tourin (Ref. 13). The agreement at 673°K is quite good over the spectral range of the measurements. However, at 1273°K the comparison is less dramatic. The shapes of the theoretical and experimental curves are very similar, with the measured and calculated values agreeing fairly well in magnitude for a total pressure of 200 mmHg. It is, however, important to notice that the experimental high temperature data show the magnitude of the emissivity to increase with decreasing total pressure. This is inconsistent with the model used here or any other available experimental results. With this single exception, all available experimental and theoretical results indicate increasing emissivity with increasing pressure. It is also interesting to note that these measurements, in this respect, are also inconsistent with each other. This is readily verified by referring to Figures 1 and 2 of the referenced paper. In particular, measurements made under identical conditions* yield in one instance a decrease of 15 to 20 percent in the emissivity near 4.3 microns as the pressure increases 14-fold, while in the other instance the emissivity increases approximately 20 percent for the same pressure increase. No mention of these inconsistencies is made other than to point out that the precision of the measurements is not very good. It was, however, noted that the 200- and 700-mm pressure curves shown in Figure 8 agree within experimental error.

At 1200°K, a comparison is shown in Figure 9 with the measurements of Oppenheim and Ben-Aryeh (Ref. 14). Figure 10 shows the results of the program compared to the experimental results of Burch and Gryvnak (Ref. 15) for pure CO_2 at 1500°K. Figure 11 again compares the program with their measurements at the same temperature for mixtures of CO_2 and N_2. Figure 12 shows a comparison of the

*In this set of measurements, only the spectral resolving power of the infrared spectrometer differed. Figure 1 indicates $\Delta\lambda = 0.018$ micron; and Figure 2, $\Delta\lambda = 0.014$ micron. Other than this the experimental conditions were apparently identical.

calculated results with the measurements of Ferrisco (Ref. 16) at 1800°K. In Figures 6 through 12 the temperature range from 300° to 1800°K has been covered indicating the present model has general validity for predicting CO_2 emissivities over a rather wide range of conditions.

At this point it should be obvious that the results of the model are highly dependent on the band parameters S and d. Since these parameters are treated as variables and simply read into the computer program, then it is a relatively easy task to modify the general program if the need arises. In particular, if better experimental data become available, the band parameters can be easily adjusted to fit these data. This is possible when two or more values of the emissivity are available at constant temperature. The calculation would simply involve writing Equation (34), the spectral emissivity equation, twice for the conditions of the measured data taken at constant temperature. The solution of this system of equations would then give the band parameters S and d.

This method will not be utilized here because of the lack of suitable experimental emissivities at the lower temperatures. Corrections to the parameters at 1500°K should necessarily involve some corrections to the interpolated values at 900°K. These values, in turn, are strongly dependent on the band parameters at 600°K which, at this point, would have to remain invariant. Thus, the values will not be altered. It would, however, be interesting to compute the parameter adjustments at one spectral point in order to determine the magnitude of the change involved. The 1500°K curves of Figures 10 and 11 at 2325 cm^{-1} were arbitrarily chosen for this. It is important to note that the equivalent path length (L_e) must not be constant for any two measurements in order to determine these parameters from experimental data. If, for example, only the total pressure varies, as in Figure 11, then only a functional relationship between the band parameters can be determined. Two independent relations would not exist for determining both S and d. This is clearly shown by by writing the emissivity equation for a particular temperature as

$$\epsilon(P_T) = 1 - \exp\left\{-KP_T f(S,d)\right\}, \tag{47}$$

where

$$f(S,d) = \left\{(1 + C_1 S)^{\frac{1}{2}} - 1\right\}/d.$$

If, however, measurements are taken with L_e treated as a variable, then

$$\epsilon\,(P_T, L_e) = 1 - \exp\left\{-KP_T f(S, d, L_e)\right\}, \tag{48}$$

where

$$f(S, d, L_e) = \left\{(1 + C_2 S L_e)^{\frac{1}{2}} - 1\right\}/d.$$

We now have available, from two or more measurements, a corresponding set of relationships, $f_1(S, d, L_{e_1})$, $f_2(S, d, L_{e_2})$, etc., for determining S and d.

To illustrate, we choose the 0.251-atm curve of Figure 11 and the 0.061-atm curve of Figure 10 at 2325 cm^{-1}.

T	1500°K	1500°K
P_T	0.061 atm	0.251 atm
L_e	7.75 cm	1.124 cm
ϵ	0.490	0.537

If we choose to calculate the band parameters in the form S/d and $S^{\frac{1}{2}}/d$, then the emissivity equation yields the two relationships

$$\frac{S}{d} = \frac{a_1 \beta_2 - a_2 \beta_1}{a_1 - a_2}, \tag{49}$$

and

$$\frac{S^{\frac{1}{2}}}{d} = \left\{\frac{a_1 \beta_2 - a_2 \beta_1}{\beta_2 - \beta_1}\right\}^{\frac{1}{2}}, \tag{50}$$

where

$$a = \frac{10}{3P_T^2 L_e}\sqrt{T/300}\left\{\ell n\left(\frac{1}{1 - \epsilon}\right)\right\}^2,$$

and

$$\beta = (P_T L_e)^{-1}\,\ell n\,(1 - \epsilon)^{-1}.$$

If the arithmetic is now carried through we obtain:

$a_1 = 117.2$ $\quad$ $a_2 = 62.41$
$\beta_1 = 1.424$ $\quad$ $\beta_2 = 2.729.$

These values give S/d = 4.22 and $S^{\frac{1}{2}}/d$ = 13.3. The tabulated values are 3.48 and 11.8 which give a percentage difference of 19 and 12 respectively, for S/d and $S^{\frac{1}{2}}/d$. The difference between the calculated and measured emissivities is approximately 10 percent in each case.

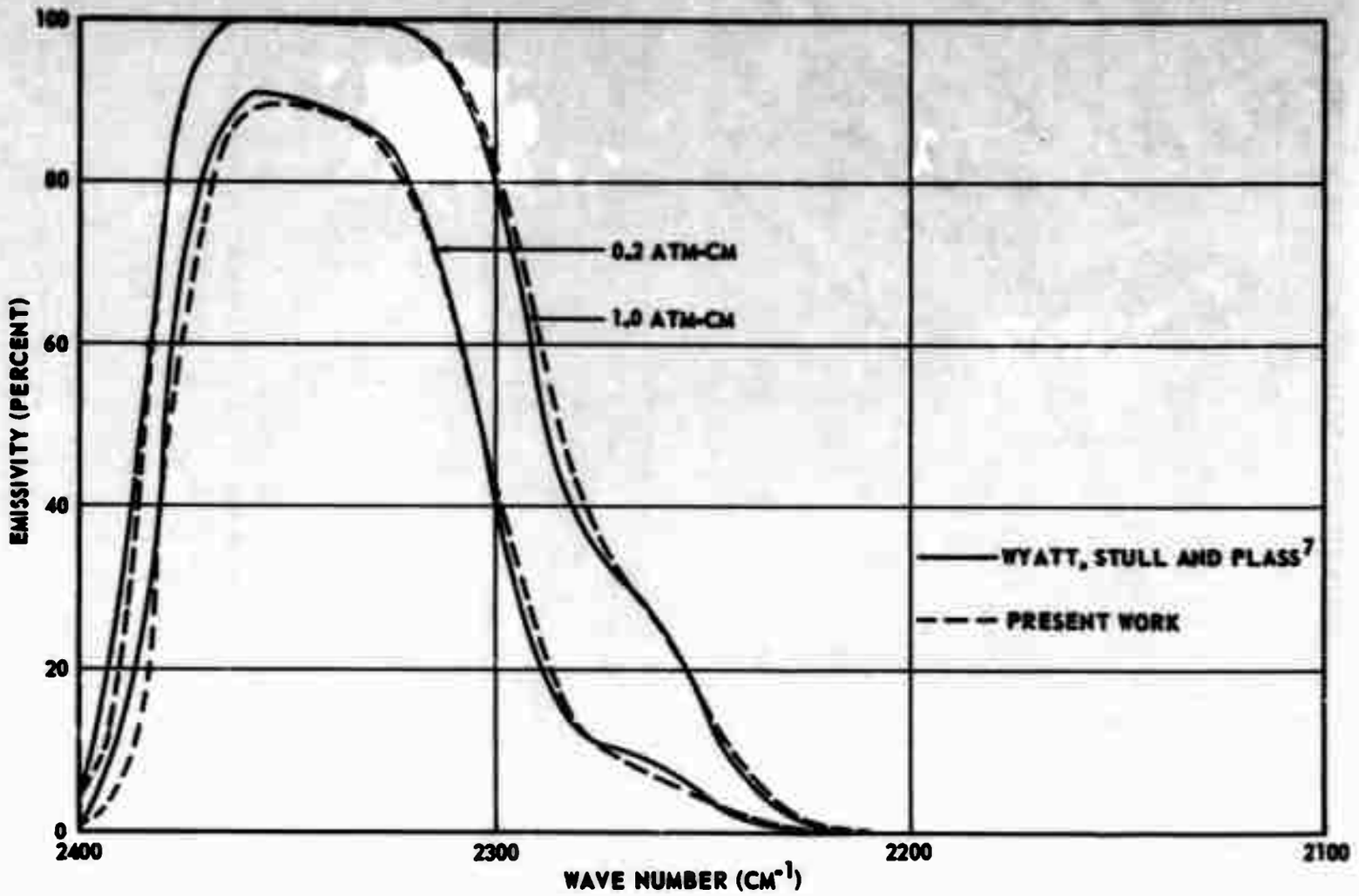

Figure 6. Spectral Emissivity of CO_2 at 300°K for a Total Pressure of 1.0 Atm

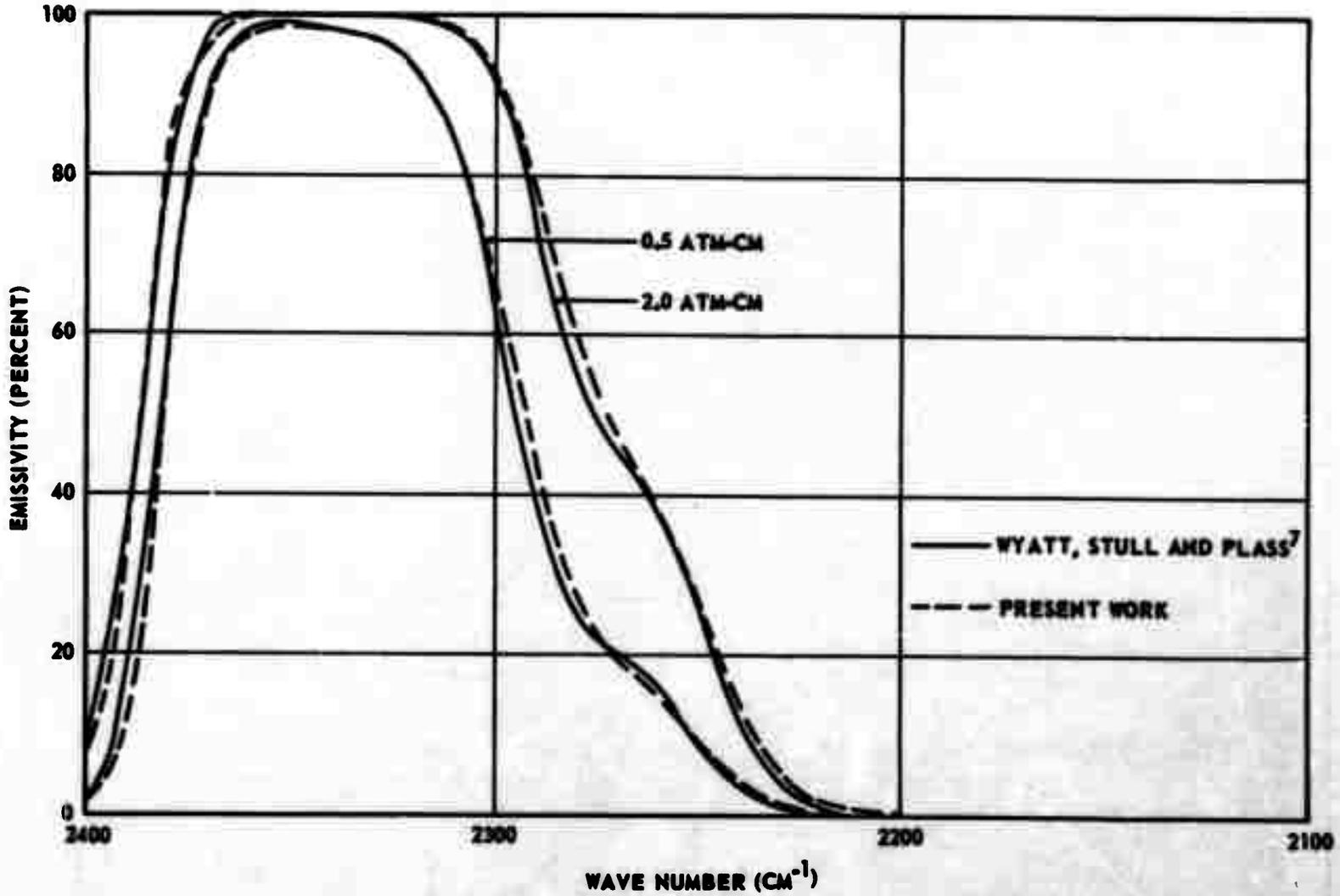

Figure 7. Spectral Emissivity of CO_2 at 300°K for a Total Pressure of 1.0 Atm

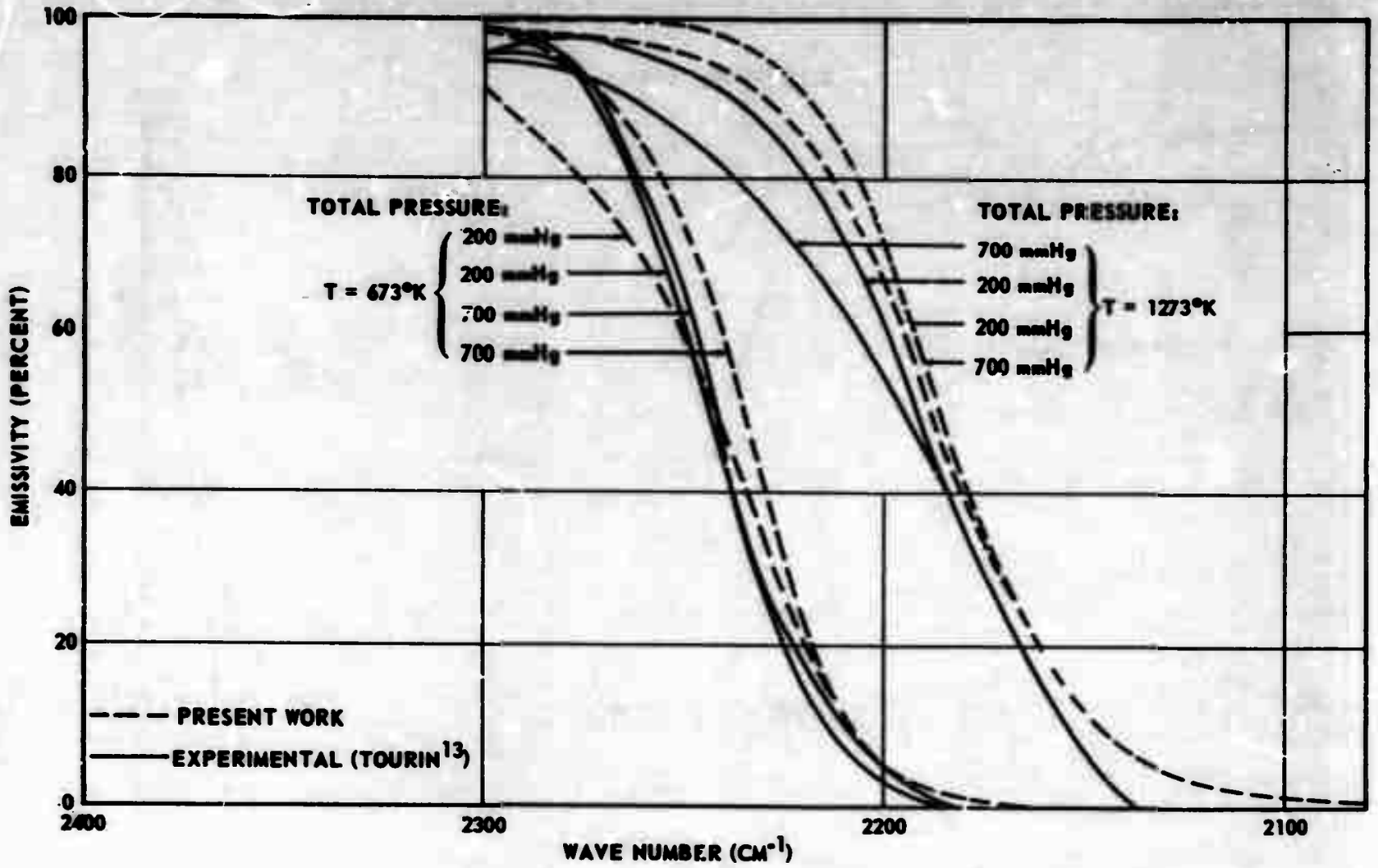

Figure 8. Spectral Emissivity of CO_2 Mixed with N_2 at 673° and 1273°K
CO_2 Concentration = 3.4 Atm-Cm

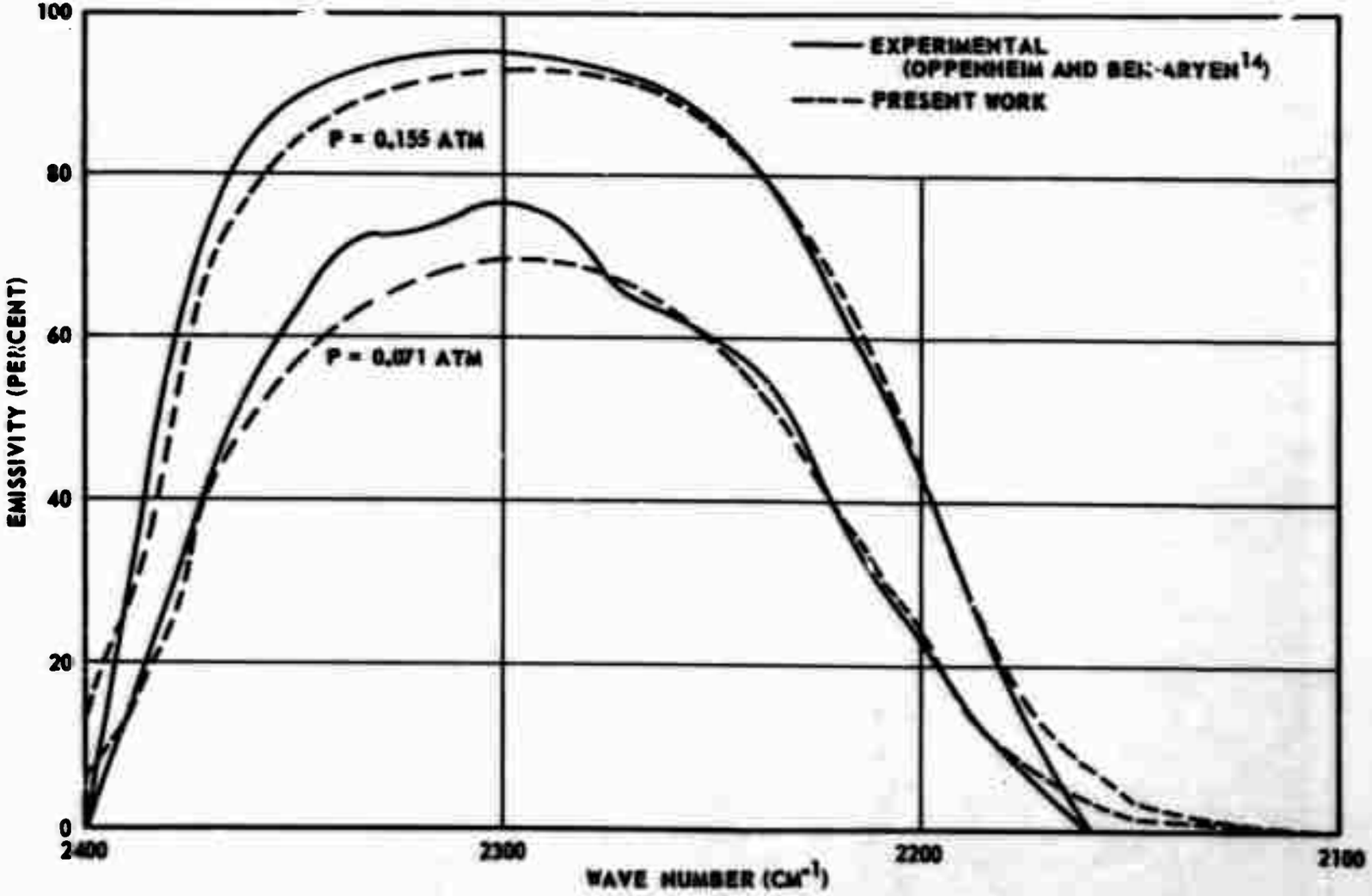

Figure 9. Spectral Emissivity of Pure CO_2 at 1200°K for an Optical Path of 15.05 Cm

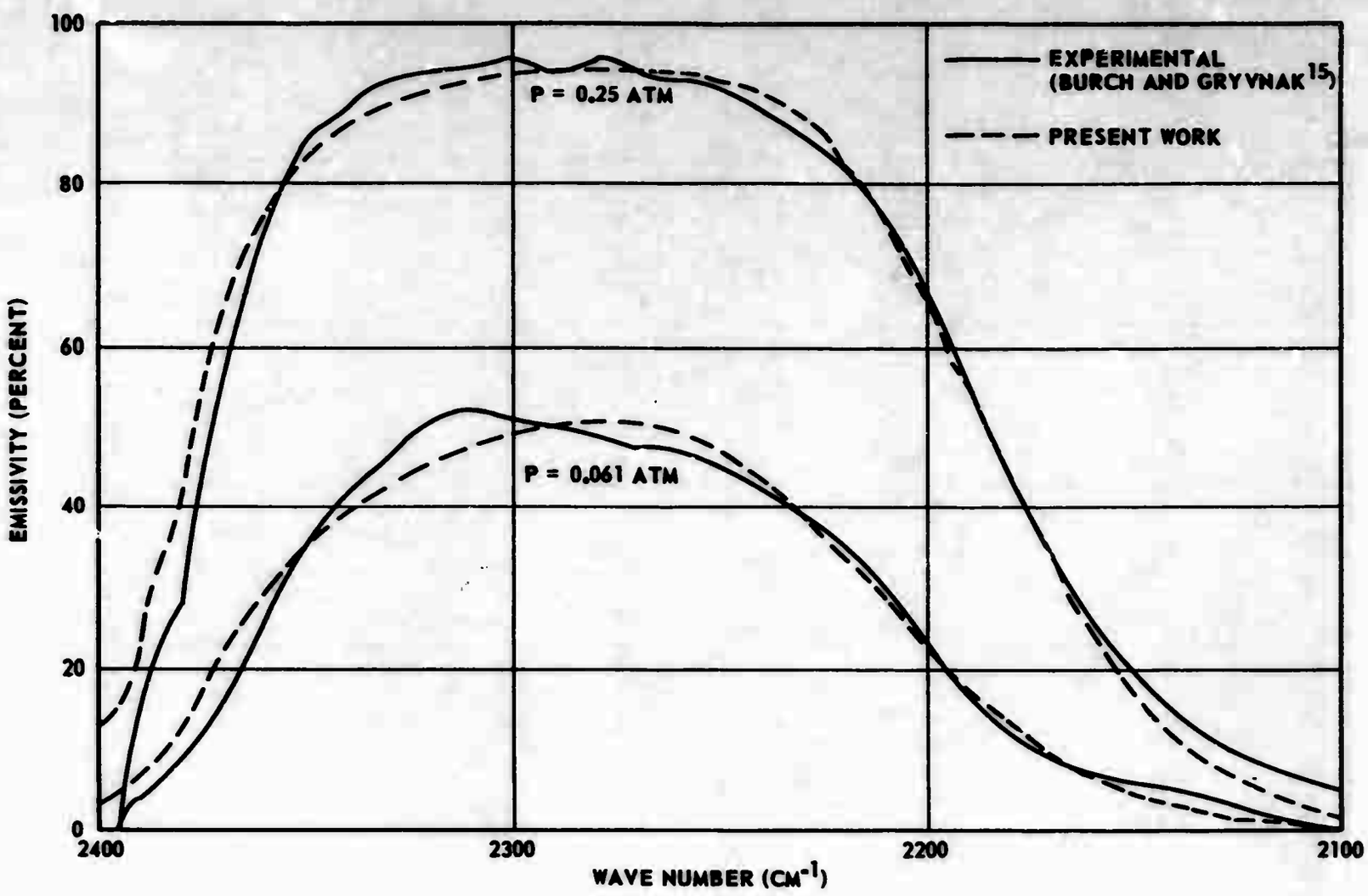

Figure 10. Spectral Emissivity of Pure CO_2 at 1500°K for an Optical Path of 7.75 Cm

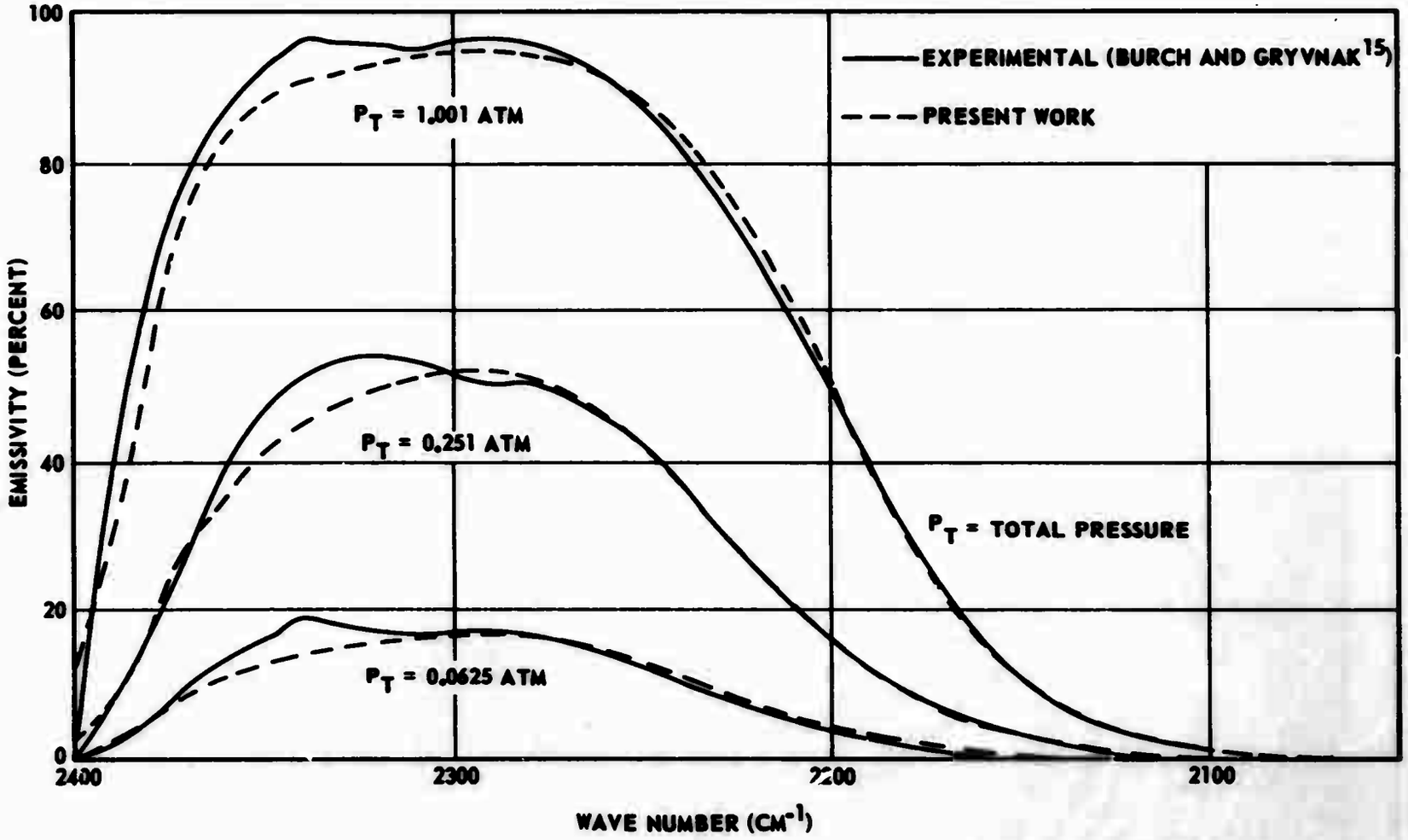

Figure 11. Spectral Emissivity of CO_2 Mixed with N_2 at 1500°K for an Optical Path of 7.75 Cm and Equivalent Optical Path of 1.24 Cm

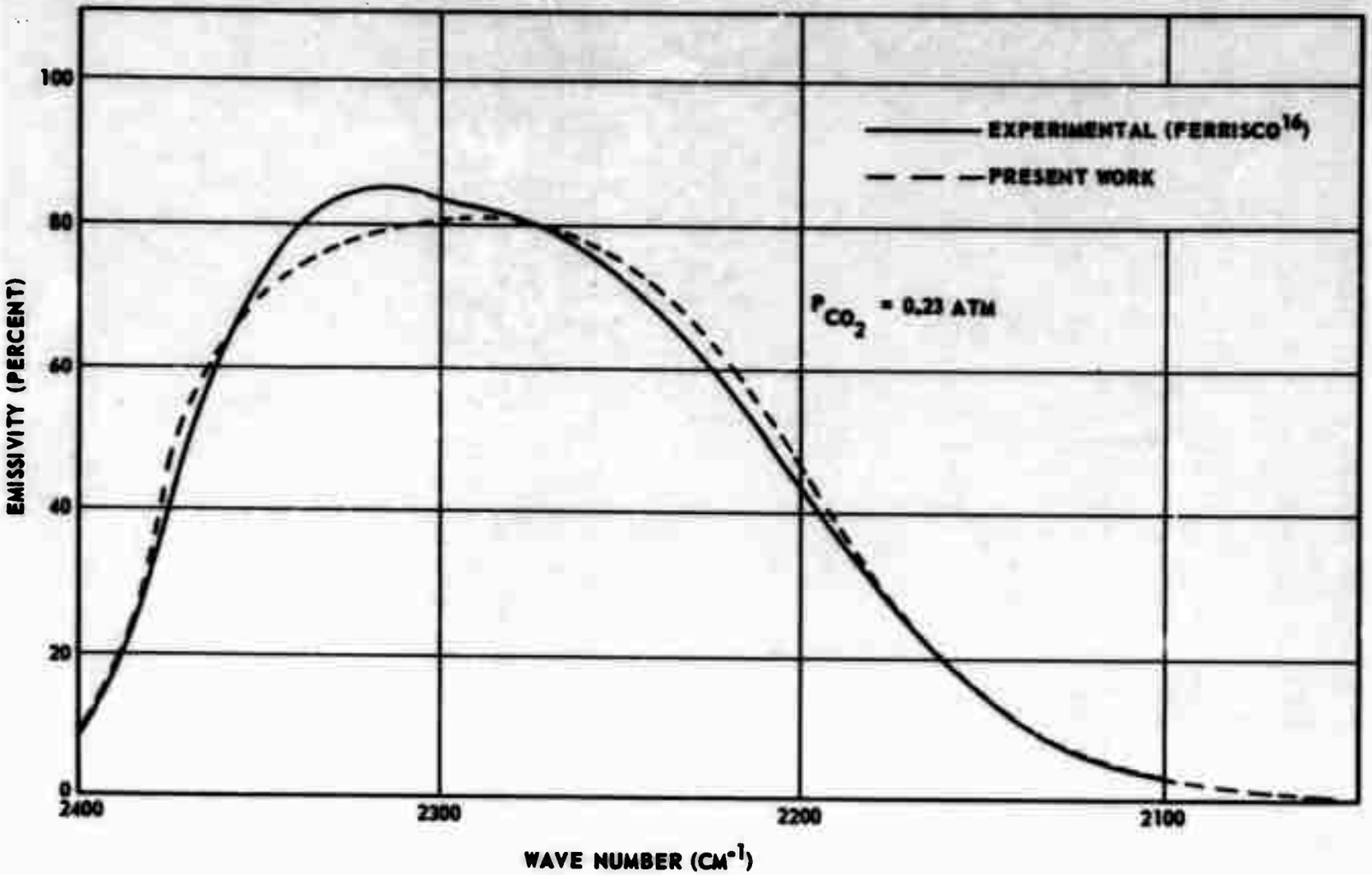

Figure 12. Spectral Emissivity of CO_2 at 1800°K for a Total Pressure of 1.0 Atm and L = 3.1 Cm

Section VIII. EMISSION CALCULATIONS

The calculation of the spectral emission or spectral radiated energy is very straightforward for a homogeneous gas after the spectral emissivity has been determined. For an inhomogeneous gas, the procedure is outlined in Section IX.

After the spectral emissivity calculations have been made, the spectral emission is obtained by multiplying the emissivity by Planck's blackbody spectral emission function. Thus, the spectral radiation is computed from the following expression

$$I_\lambda = \frac{C_1 \lambda^{-5} \epsilon(\lambda, T, x)}{\pi \left[\exp(C_2/\lambda T) - 1\right]} \quad \frac{\text{watts}}{\text{cm}^2\text{-micron-steradian}}, \qquad (51)$$

where

$C_1 = 37,413$ watts/micron^4-cm^{-2}-steradian^{-1},
$C_2 = 14,388$ microns-°K;

and T is expressed in °K and λ in microns.

The coordinate x in the above expression measures the thickness of the radiating gas in a direction parallel or along the direction in which it is desired to determine the emitted radiation. The total spectral radiation is then obtained by multiplying Equation (51) by the projected surface area normal to the direction in which it is desired to make the calculation, i.e., normal to the thickness coordinate x. Figure 13 shows the results of such a calculation for the conditions indicated. The dotted curves represent the radiation emitted from a blackbody of the same temperature.

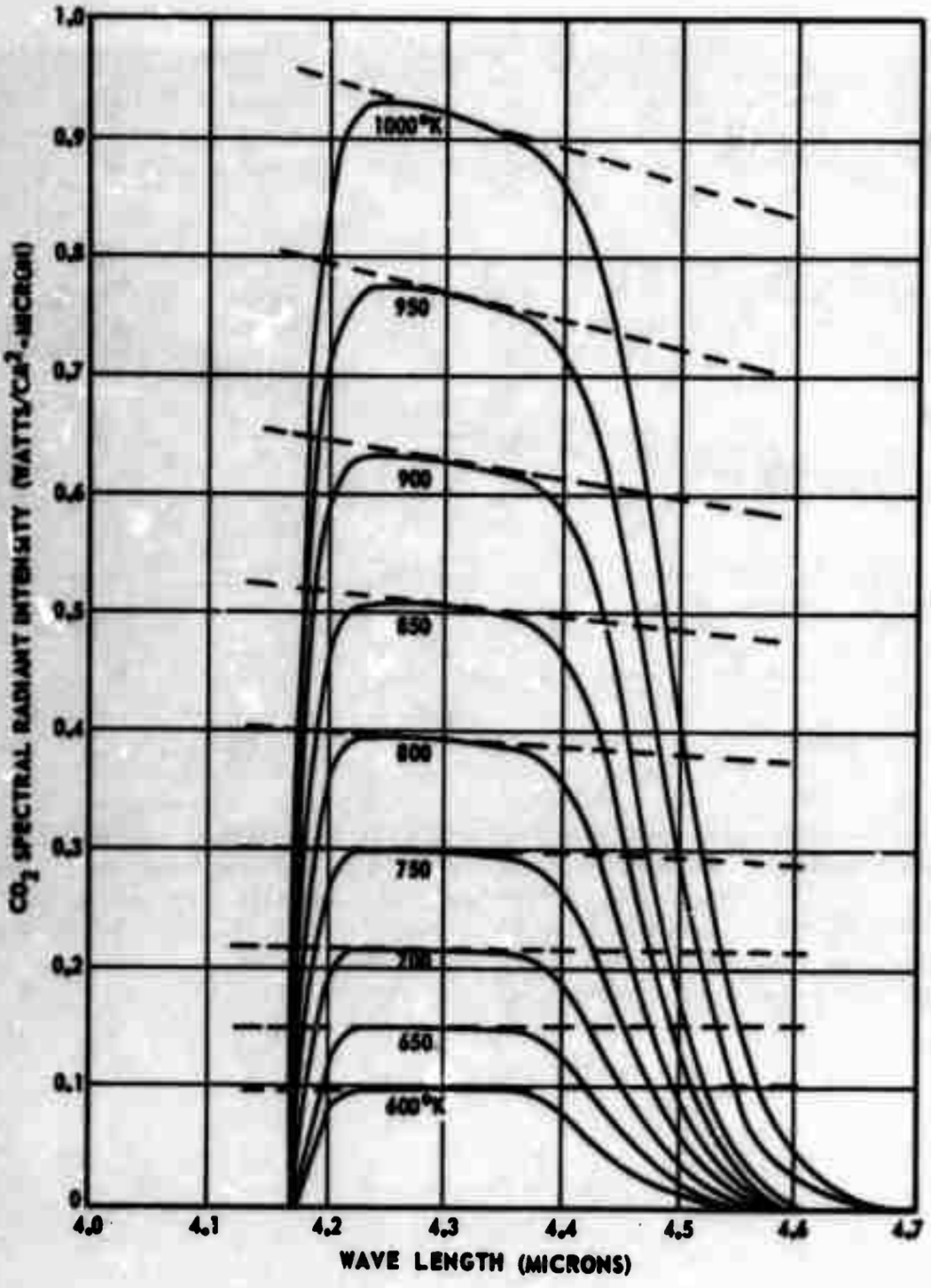

Figure 13. Spectral Emission Curves for CO_2 at Various Temperatures for a Total Pressure of 1.0 Atm and an Equivalent Path of 2.0 Cm

Section IX. INHOMOGENEOUS CALCULATIONS

The calculation of the radiation emitted from a gaseous system that possesses both temperature and concentration gradients is considerably more difficult than for a homogeneous system. The problem can be approached by means of the Curtis-Godson approximation. In essence, this method takes an inhomogeneous gas which has a given transmittance and replaces it with a homogeneous gas which has the same transmittance. This is accomplished mathematically by computing an equivalent set of band parameters for the inhomogeneous gas (Ref. 17). The procedure is formulated by dividing the nonhomogeneous gaseous mixture into several segments, each of which can be considered to be a zone of constant properties. After the transmittance has been computed, the emissivity and corresponding radiation can then be calculated for each homogeneous segment and transmitted through the appropriate inhomogeneous thickness to determine the emission. The total emission is obtained by repeating this for each segment and summing the results.

The mathematical formulation for the inhomogeneous calculations will now be formulated. Let X denote a geometrical thickness of the inhomogeneous radiating gas. We let $P_s(X)$ denote the concentration or partial pressure of the radiating constituent. The optical depth is defined as

$$W(X) = \int_0^X P_s(X)dX, \tag{52}$$

where the outer surface of the emitting gas is denoted by the coordinate $X = 0$. For a homogeneous mixture the transmission is assumed to be given by $1 - \epsilon$, which from Equation (34) is

$$\tau = \exp - \left\{ \frac{2\gamma}{d} \left(\sqrt{1 + \frac{SW}{\gamma}} - 1 \right) \right\}, \tag{53}$$

where $W = P_s X$ and $\gamma = \alpha P_T$.

Let us now define the two quantities

$$\beta = \frac{SW}{d} \quad \text{and} \quad \psi = \frac{(S\frac{1}{2})}{d} \gamma W.$$

Then

$$\frac{\psi}{\beta} = \frac{\gamma}{d} \text{ and } \frac{\beta^2}{\psi} = \frac{SW}{\gamma}.$$

The equation for the homogeneous transmission then becomes

$$\tau = \exp - \left\{ \frac{2\gamma}{\beta} \left(\sqrt{1 + \frac{\beta^2}{\psi}} - 1 \right) \right\}. \tag{54}$$

For the inhomogeneous gas, we now replace the quantities β and ψ in the above expression by equivalent quantities defined by the equations

$$\beta_e = \left(\frac{S}{d} W \right)_e = \int_0^{W(X)} \frac{S}{d}(W)\, dW, \tag{55}$$

$$\psi_e = \left(\frac{S}{d^2} W \right)_e = \int_0^{W(X)} \frac{S}{d^2}(W)\, \gamma(W)\, dW. \tag{56}$$

Thus, $\beta_e = \beta_e(X)$ and $\psi_e = \psi_e(X)$ for specified distributions $T = T(X)$, $P_s = P_s(X)$, and $P_T = P_T(X)$.

In order to illustrate the preceding discussion, a typical example calculation will be carried through analytically. Assume that

$$T = T_o e^{X/a}$$

$$P_s = P_{s_o} e^{X/b}$$

$$P_T = C(\text{constant}).$$

Then

$$W(X) = \int_0^X P_s(X)\, dX = b P_{s_o} (e^{X/b} - 1).$$

This can be rewritten in the form $X = X(W)$. Let us choose to write

$$e^X = \left(1 + \frac{W}{b P_{s_o}} \right)^b.$$

Then the temperature T can be expressed as $T = T(W)$,

$$T = T_o \left(1 + \frac{W}{bP_{s_o}}\right)^{b/a}.$$

For a particular spectral point, let us now assume that both S/d and S/d^2 can be expressed as

$$S/d = C_1 + C_2T + C_3T^2,$$

$$S/d^2 = C_4 + C_5T + C_6T^2,$$

where $T_o \leq T \leq T_{max}$. Since T has been expressed as $T = T(W)$, then

$$S/d = C_1 + C_2T_o \left(1 + \frac{W}{bP_{s_o}}\right)^{b/a} + C_3T_o^2 \left(1 + \frac{W}{bP_{s_o}}\right)^{2b/a}$$

with a similar expression for S/d^2.

Also since

$$\beta_e = \int_0^{W(X)} \frac{S}{d}(W)dW,$$

then carrying through the integration and simplifing gives

$$\beta_e = a_1\left(e^{X/\epsilon_1} - 1\right) + a_2\left(e^{X/\epsilon_2} - 1\right) + a_3\left(e^{X/\epsilon_3} - 1\right)$$

with

$$\epsilon_1 = b$$

$$\epsilon_2 = ab/(a + b)$$

$$\epsilon_3 = ab/(a + 2b)$$

$$a_1 = P_{s_o}\epsilon_1 C_1$$

$$a_2 = P_{s_o}\epsilon_2 C_2 T_{o_2}$$

$$a_3 = P_{s_o}\epsilon_3 C_3 T_o.$$

A similar calculation for ψ_e gives

$$\psi_e = \eta_1 (e^{X/\nu_1} - 1) + \eta_2 (e^{X/\nu_2} - 1) + \eta_3 (e^{X/\nu_3} - 1)$$

with

$$\nu_1 = 2ab/(2a - b)$$

$$\nu_2 = 2ab/(2a + b)$$

$$\nu_3 = 2ab/(2a + 3b)$$

$$\sigma = 0.075 \sqrt{300}\, P_{s_o}/\sqrt{T_o}$$

$$\eta_1 = \sigma \nu_1 C_4$$

$$\eta_2 = \sigma \nu_2 C_5 T_{o_2}$$

$$\eta_3 = \sigma \nu_3 C_6 T_o \cdot$$

Figure 14 shows the transmission as a function of gas thickness for a specified set of conditions.

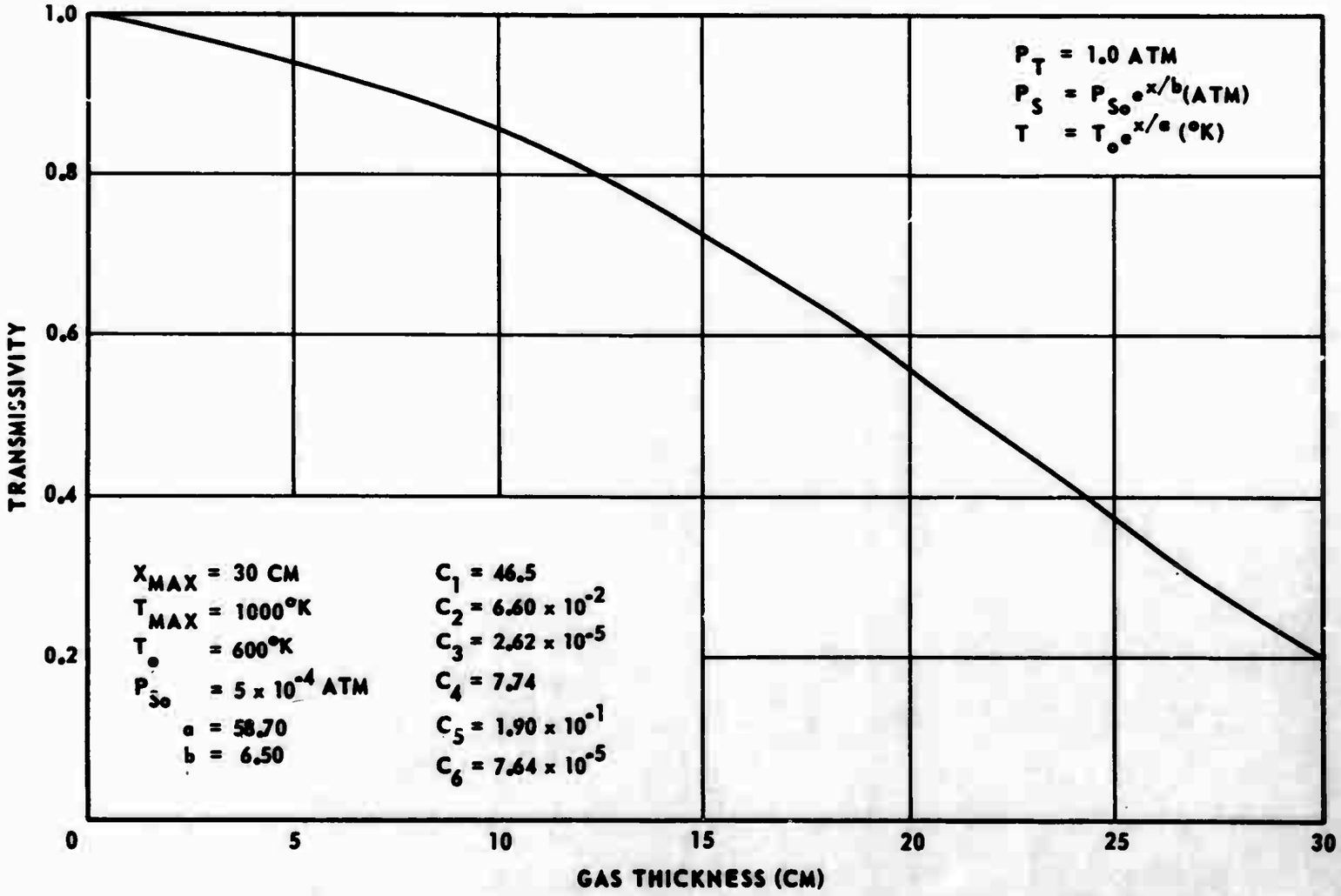

Figure 14. Transmission Versus Gas Thickness for an Inhomogeneous Gas

Section X. SUMMARY

The use of the statistical model combined with the curve of growth relationship introduced by Malkmus leads to a very satisfactory model for the calculation of CO_2 emission in the 4.3-micron band. The model is very attractive in the sense that the use of theoretically determined spectroscopic parameters yield emissivity values which agree with experimental results to within a few percentages over the range of variables considered. Reliable experimental data can then be used to refine the parameters to produce even better results.

It should also be noted that the simplest of all relations has been assumed to exist between the equivalent and total pressure of the gaseous system—namely, $P_e = P_T$. Other relationships have been proposed for gaseous mixtures (see Ref. 4 for a brief discussion of this). However, this assumption leads to very good results for the CO_2 concentrations considered in this study.

It was mentioned in the introduction that a salient feature of this program was to develop a computerized computational scheme which could be readily integrated into a flow-field calculation. With minor exceptions, this phase of the work has also been completed. Preliminary results which have been completed for computing jet plume emissions indicate that reasonably good agreement is obtained between the predicted analytical results and experimental measurements.

As a final item of interest, Figure 15 shows the results of the program for a particular jet plume along with the actual normalized measured data. Since the measured data were obtained at a distance of 550 feet from the radiating source, the theoretical data were transmitted through an equivalent atmospheric path (Ref. 18). The agreement is remarkably good when it is considered that one set of the data is purely analytical, i.e., temperature and CO_2 concentrations for the jet, which are highly nonhomogeneous, as well as the radiation calculation itself.

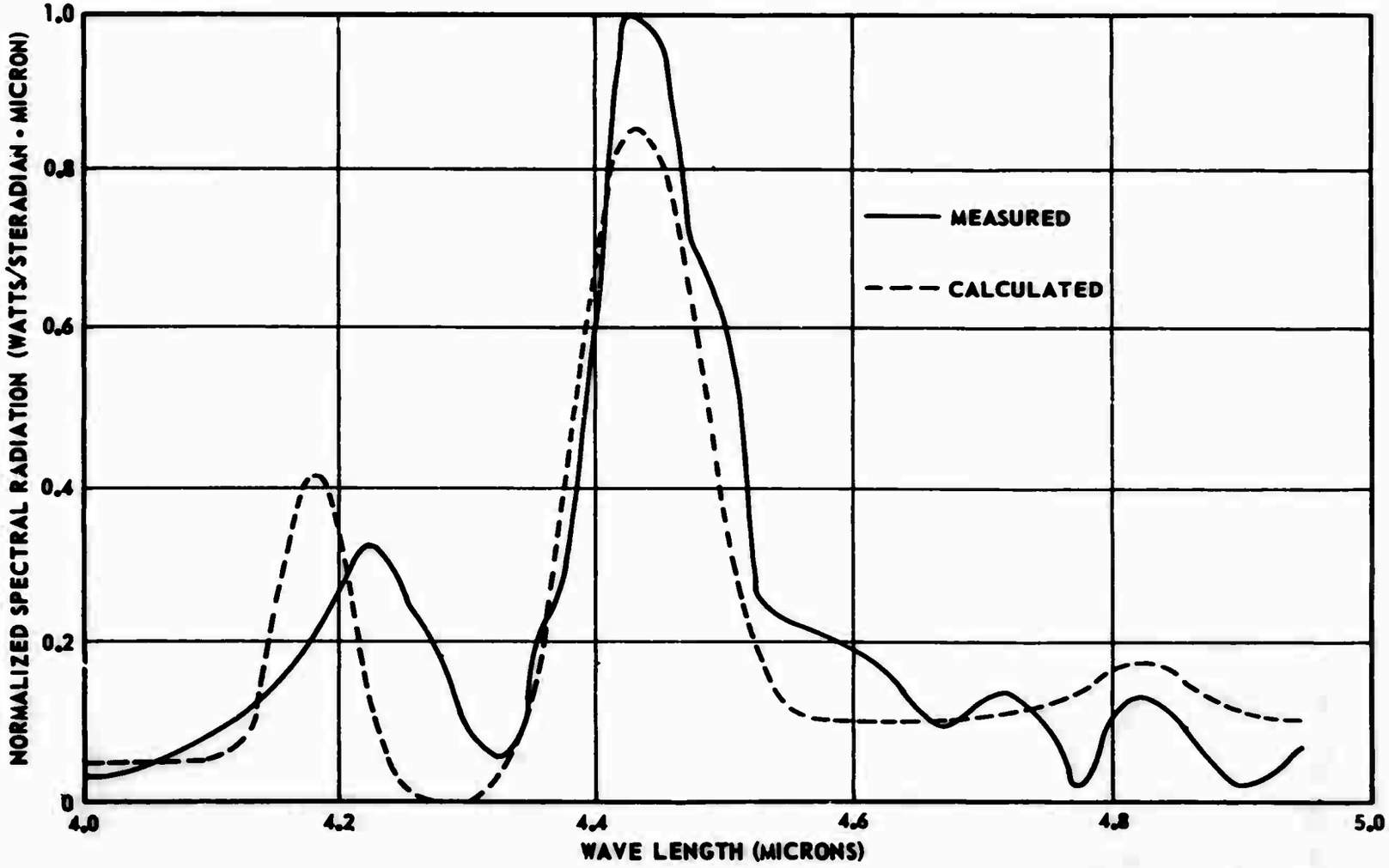

Figure 15. Comparison of Predicted and Measured Spectral Emission for a Particular Jet Plume

Next page omitted,
no information deleted.

REFERENCES

1. G. Herzberg, Spectra of Diatomic Molecules, Van Nostrand, Princeton, New Jersey (1950).

2. G. N. Plass, J. Opt. Soc. Am. 48, 690 (1958).

3. Handbook of Military Infrared Technology, edited by W. L. Wolfe, U. S. Government Printing Office, Washington, D. C. 20402 (1965).

4. D. E. Burch, E. B. Singleton, and D. Williams, Appl. Opt. 1, 359 (1962).

5. L. D. Gray, J. Quant. Spectry. Radiative Transfer 5, 569 (1965).

6. Y. Ben-Aryeh, Appl. Opt. 6, 1049 (1967).

7. V. R. Stull, P. J. Wyatt, and G. N. Plass, Infrared Transmission Studies, Final Rpt. Vol. III, "The Infrared Absorption of Carbon Dioxide," 55D-TDR-62-127, Space Systems Division, Air Force Systems Command, Los Angeles, California (31 January 1963).

8. W. Malkmus, J. Opt. Soc. Am. 53, 951 (1963).

9. R. Ladenburg u. F. Reiche, Ann. Physik 42, 181 (1913).

10. Handbook of Mathematical Functions, edited by M. Abramowitz and I. A. Stegun, Applied Math Series, 55, U. S. Government Printing Office, Washington, D. C. 20402 (1966).

11. Study on Exhaust Plume Radiation Predictions, Interim Progress Report, General Dynamics, Space Science Laboratory, Report No. GD/C-DBE-66-001, Contract NAS 8-11363 (January 1966).

12. G. N. Plass, J. Opt. Soc. Am. 53, 951 (1963).

13. R. H. Tourin, J. Opt. Soc. Am. 51, 175 (1961).

14. U. P. Oppenheim and Y. Ben-Aryeh, J. Opt. Soc. Am. 53, 344 (1963).

15. D. E. Burch and D. A. Gryvnak, Infrared Radiation Emitted by Hot Gases and Its Transmission Through Synthetic Atmosphere, Sci. Rpt. No. U-1929, Ford Motor Company, Aeronutronic Division.

16. C. C. Ferrisco, High Temperature Infrared Emission and Absorption Studies, Astronautics Report AE 61-0910 (September 1961).

17. B. Krakow, H. J. Babrov, G. J. Maclay, and A. L. Shabott, Appl. Opt. 5, 1791 (1966).

18. W. D. Hyman and D. H. Dublin, Report No. RE-TM-68-5, A Computer Program for Infrared System Analysis, U. S. Army Missile Command, Redstone Arsenal, Alabama 35809 (September 1968).

UNCLASSIFIED

Security Classification

DOCUMENT CONTROL DATA - R & D

(Security classification of title, body of abstract and indexing annotation must be entered when the overall report is classified)

1. ORIGINATING ACTIVITY (Corporate author) Advanced Sensors Laboratory Research and Engineering Directorate (Provisional) U. S. Army Missile Command Redstone Arsenal, Alabama 35809	2a. REPORT SECURITY CLASSIFICATION Unclassified 2b. GROUP

3. REPORT TITLE

A MODEL FOR THE SPECTRAL EMISSIVITY OF CARBON DIOXIDE IN THE 4.3-MICRON BAND

4. DESCRIPTIVE NOTES (Type of report and inclusive dates)

5. AUTHOR(S) (First name, middle initial, last name)

H. Tracy Jackson, Jr.

6. REPORT DATE 7 April 1969	7a. TOTAL NO. OF PAGES 65	7b. NO. OF REFS 18
8a. CONTRACT OR GRANT NO. b. PROJECT NO. (DA) 1522901A204 AMC Management Structure Code No. c. 5221.11.146 d.	9a. ORIGINATOR'S REPORT NUMBER(S) RE-TR-69-9 9b. OTHER REPORT NO(S) (Any other numbers that may be assigned this report) AD_____	

10. DISTRIBUTION STATEMENT

This document is subject to special export controls and each transmittal to foreign governments or foreign nationals may be made only with prior approval of this Command, Attn: AMSMI-RE.

11. SUPPLEMENTARY NOTES	12. SPONSORING MILITARY ACTIVITY Same as No. 1

13. ABSTRACT

This report describes in somewhat tutorial detail a method for computing the spectral emissivity of hot carbon dioxide in the 4.3-micron band. This band is taken to cover the spectral region 2050 to 2400/cm^{-1} (4.17 to 4.88 microns). Data are presented for the temperature range 300° to 2100°K. Spectroscopic band parameters have largely been taken from available literature data. The average values for the integrated intensity of a rotational line (S) and the distance between the spectral lines (d) are tabulated in the standard form S/d and $S^{\frac{1}{2}}/d$. Values are listed every 5/cm^{-1} in increments of 300°K.

Emissivities are calculated by the statistical model. A curve of growth function suggested by Malkmus and adopted by Ben-Aryeh is used for the relationship between absorption and reduced path lengths. The results of this model agree most favorably with reliable experimental measurements.

The discussion includes homogeneous as well as inhomogeneous gases. The homogeneous case is presented in its entirety in that the emissivity model, the molecular band parameters, and the digital computer program are presented. Illustrative examples are given for both the homogeneous and inhomogeneous formulations.

DD FORM 1 NOV 68 1473 REPLACES DD FORM 1473, 1 JAN 64, WHICH IS OBSOLETE FOR ARMY USE.

UNCLASSIFIED

Security Classification

14. KEY WORDS	LINK A		LINK B		LINK C	
	ROLE	WT	ROLE	WT	ROLE	WT
Spectral emissivity						
Molecular parameters						
Emissivity program						
Radiant intensity						
Inhomogeneous gases						
Mathematical model						
Homogeneous gases						